Protein−Sugar-Glass Nanoparticle Platform for the Development of Sustained-Release Protein Depots by Overcoming Protein Delivery Challenges

Poulomi Polley,[†] Shivam Gupta,[†,§] Ruby Singh,[†] Arpan Pradhan,[‡] Suparna Mercy Basu,[†] Remya V.,[†] Sunil Kumar Yadava,[†] and Jyotsnendu Giri*,[†]

[†]Department of Biomedical Engineering, Indian Institute of Technology Hyderabad, Kandi 502285, Telangana, India

[‡]Department of Biosciences and Bioengineering, Indian Institute of Technology Bombay, Powai, Mumbai 400076, Maharashtra, India

[§]Department of Bioengineering, School of Engineering, The University of Tokyo, Tokyo 113-8654, Japan

S *Supporting Information*
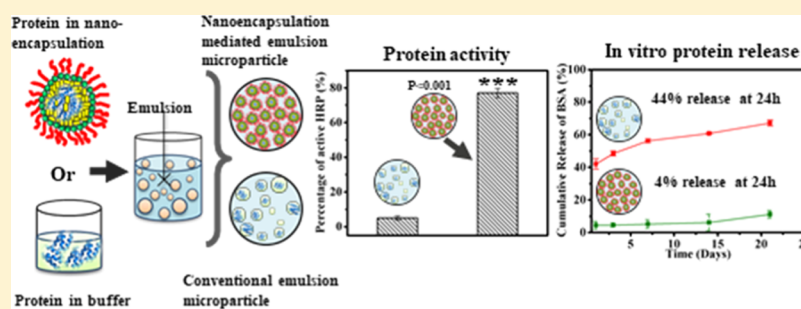
ABSTRACT: Therapeutic protein depots have limited clinical success because of the presence of critical preparation barriers such as low encapsulation, uncontrolled release, and activity loss during processing and storage. In the present study, we used our novel protein-nanoencapsulation (into sugar-glass nanoparticle; SGnP) platform to prepare a protein depot to overcome the abovementioned formidable challenges. The SGnP-mediated microparticle protein depot has been validated using four model proteins (bovine serum albumin, horseradish peroxidase, fibroblastic growth factor, and epidermal growth factor) and model biodegradable poly(lactic-*co*-glycolic acid) polymer system. The results show that our protein-nanoencapsulation-mediated platform provides a new generic platform to prepare a protein depot through the conventional emulsion method of any polymer and single/multiple protein systems. This protein depot has the required pharmaceutical properties such as high encapsulation efficiency, burst-free sustained release, and protein preservation during processing and storage, making it suitable for off-the-shelf use in therapeutic protein delivery and tissue engineering applications.

KEYWORDS: protein depot, protein nanoencapsulation, double emulsion, microparticles, protein delivery, protein therapeutics, tissue engineering

1. INTRODUCTION

Advances in production strategies and technological progress in the field of biotechnology have created a surge in the availability of therapeutic protein molecules.[1,2] These molecules are attractive candidates over small molecules due to their high target specificity and efficacy with low off-target effects with normal biological processes. With proteins being labile in a physiological environment and having a short half-life, the current protein therapy standard of care requires frequent subcutaneous injections (few times a week or daily).[3,4] This leads protein therapy to have poor patient compliance and is expensive due to higher than desired doses.[1−4] Therefore, there is an unmet clinical need to develop sustained-release formulation or protein depot to improve patient compliance and efficacy and make the protein therapy cost-effective.[5] Microparticulate formulations of protein depot

for long-term controlled release of active therapeutic protein have immense clinical importance for the treatment of many diseases, conditions, and regeneration of specific tissues.[6−11] Despite the high potential of biodegradable polymer-based depots, clinical success has been limited for few small molecules and peptide/protein formulation due to the presence of critical barriers such as low encapsulation efficiency, uncontrolled release, and activity loss during processing and storage.[12−14] The known example is Nutropin Depot, a sustained delivery system of recombinant human growth hormone (rhGH) encapsulated into biodegradable

poly(lactic acid-*co*-glycolic acid) (PLGA) microspheres, approved by the US FDA in 1999 as a monthly injection formulation.[15,16] It was withdrawn from the market in 2004 due to several issues, such as relatively low loading leading to frequent injections of a large amount of PLGA carrier, high burst release, protein denaturation during processing and after administration, and adverse reactions.[17−20]

Various microencapsulation methods have been developed over the past decades, including emulsion method,[21] phase separation (coacervation),[22,23] spray drying,[24] spray freeze drying,[25,26] and supercritical fluid technology.[27,28] However, only emulsion methods, coacervation, and spray drying have reached large-scale production of PLGA-based protein depots.[29] Among these methods, the emulsion-based methods, for example, water−oil−water (w−o−w) and solid−oil−water (s−o−w) are common for the preparation of a protein delivery system or depot in pharmaceutical industries mainly due to their easy scalability and simplicity.[6,30−33] In this process, protein molecules undergo several process-related stresses, such as, elevated temperature, high mechanical agitation, and organic−aqueous interfaces, which leads to significant protein activity loss.[10,11,34−37] Moreover, this process is also associated with low protein encapsulation, frequently burst release, and low storage stability of the entrapped protein.[38] Sufficient shelf life of the microparticle depot is essential for their clinical application, particularly for transport and storage until their use. Over the last two decades, various approaches developed have tried to overcome each of the above mentioned challenges individually or in combination. Interface stabilizers,[39,40] protein crystallization,[41] and covalent protein modification[42] have been used to ameliorate the impact of individual stresses in emulsion-based methods. Similarly, approaches such as coencapsulation of lyoprotectant and antacid $[Mg(OH)_2]$ have been used to tune the polymer−protein microenvironment to improve stability of proteins.[43,44] However, these approaches provide excellent process-related protein stability with the expense of huge burst release of protein.[43,44] Similarly, several novel approaches such as remote-loading and self-healing micro-pores were developed to improve protein stability and burst release, respectively.[10,45,46] The former, remote-loading of protein, is specific to the polymer and protein system. Although there are many approaches to overcome one aspect of performance, they remain neutral or harmful to the other.[10,11,32,44−46] In addition to these trade-offs in the performance,[44,45] many approaches developed are specific to the polymer or protein system,[45] which will need a different approach for new therapeutic protein. Despite significant progress over the last 10−15 years on the development of control release systems of large molecules (protein) from PLGA and related polymers, obstacles such as protein stability, manufacturing, and microencapsulation issues are yet to be overcome simultaneously.[10] Ideally, there is a need for a single approach that will ameliorate all stresses related to the emulsion method resulting in high encapsulation efficiency and storage stability, while giving a burst-free sustained release for any protein and polymer system of interest.

Recently, we have developed a novel technique of nanoencapsulation of protein into a sugar-glass matrix to make a protein−sugar-glass nanoparticle system (SGnP) as an all-in-one solution to overcome challenges related to protein encapsulation and delivery from nanofiber polymer scaffold for tissue engineering applications.[47,48] SGnP was prepared by

rapid quenching of inverse micelles of a protein−excipient-aqueous suspension in isooctane stabilized by sodium 1,4-bis(2-ethylhexoxy)-1,4-dioxobutane-2-sulfonate (AOT) to 77 K (liquid nitrogen) to obtain a glassy matrix of sugar. In the SGnP system (20 to 160 nm), protein is sequestrated in a glassy matrix of sugar and excipients for stabilization of protein and surfactant (AOT) coating provides efficient dispersion into any polymer system of interest. In our previous studies, we have shown that water: surfactant mole ratio (w = $[H_2O]/$ $[AOT]$) determined the equilibrium micelle size and could be varied (from 10 to 15) to get the desired size of SGnP within 20 and 160 nm. Similarly, the mass ratio of protein to trehalose used was 1:500 to provide sufficient coating of trehalose on the protein during processing. In previous studies, various growth factors (GF) were encapsulated (up to 2% w/w) into nanofibers using the SGnP system. However, in case of the microparticle protein depot, large loading capacity of protein in the microparticle matrix will be beneficial for long-term delivery of therapeutic protein. To achieve high loading-capacity microparticles, one can think of increasing the amount of protein−SGnP into microparticles, but the amount of protein−SGnP should be limited due to possible formation of nanoporous polymer matrix at high loading of SGnP and may result in burst release of protein. On the other hand, use of SGnP with increased number of protein molecules in each nanoparticles can be used to load higher amount of protein into the microparticle protein depot, which demands modification of our previously reported SGnP system. We hypothesized that the modification of SGnP system with high protein molecules by reducing the ratio of trehalose/protein as well as decreasing the size of the SGnP (increase nano-confinement of protein) will allow us to develop a protein depot with high protein-loading capacity for sustained-release applications. In the present study, we have further explored our novel SGnP system to encapsulate a higher amount of protein into the polymer microparticle system to prepare the protein depot. To test our hypothesis, modified SGnP system with various model proteins were prepared, and the model proteins were encapsulated into PLGA [poly(lactic-*co*-glycolic acid)] polymer microparticles using protein-in-buffer and protein-in-SGnP representing conventional emulsion methods (water-in-oil-in-water; w−o−w and water-in-oil-in-oil; w−o−o) and our nanoencapsulation method, respectively.

To check the generic nature of the SGnP platform, we have used four model protein systems (namely bovine serum albumin; BSA, horseradish peroxidase; HRP, fibroblastic growth factor; FGF-2, and epidermal growth factor; EGF) encapsulated into a model biodegradable polymer. Encapsulation efficiency, release profile, process, and storage stability of proteins were thoroughly studied comparatively between the conventional protein encapsulation methods (protein in buffer) and our SGnP-mediated protein encapsulation. Finally, the ex vivo functionality of SGnP-mediated dual protein-loaded protein depots was confirmed by their ability to facilitate "cancer stem cell mammosphere" formation. Our study indicates that the SGnP system provides a new platform to prepare microparticle protein depot through the conventional emulsion method (w−o−w) of PLGA/similar polymer and protein (single and multiple) systems with required pharmaceutical properties such as high loading capacity, burst-free sustained release, and protein preservation during processing and storage for therapeutic applications.

2. MATERIALS AND METHODS

2.1. Materials. PLGA (lactide/glycolide; 50:50, MW, 17 kDa) was purchased from Evonik (Germany). Poly(vinyl alcohol) (PVA) MW 50 000−90 000 was purchased from Alfa Aesar, India. BSA, fluorescein isothiocyanate-conjugated BSA (FITC−BSA), surfactants Tween 20, Span 80, and sodium 1,4-bis(2-ethylhexoxy)-1,4-dioxobutane-2-sulfonate (AOT) were purchased from Sigma-Aldrich (India). HRP and *o*-phenylenediamine dihydrochloride (OPD) substrate were supplied by Sisco Research Laboratories Pvt. Ltd., India. Analytical grade reagents, light paraffin oil, hydrogen peroxide, and organic solvents dichloromethane (DCM), isooctane, and *n*-hexane were purchased from Sisco Research Laboratories Pvt. Ltd. (Mumbai, India). EGF, bFGF-2, and ELISA kit for FGF-2 quantification were obtained from Peprotech, USA, and B27 supplement was purchased from Gibco. Micro BCA Protein Assay Kit and NanoOrange Protein Quantification Kit were obtained from Thermo Fisher Scientific (USA). Cell lines: MCF 7 (human breast carcinoma) and human gingival fibroblasts (HGF) were procured from ATCC, USA.

2.2. Methods. *2.2.1. Preparation of Dye/Protein-Encapsulated Sugar-Glass Nanoparticles (SGnPs). 2.2.1.1. Protein-Encapsulated SGnP.* Model proteins BSA, HRP, FGF-2, and EGF were individually encapsulated into SGnPs following similar processes as described in our previous publication.[47] In brief, aqueous phases (0.85 to 0.95 mL) containing protein and other protein-specific excipients were added into 12 mL of isooctane pre-equilibrated with 0.4 mol/L solution of AOT in a 25 mL centrifuge tube. The mixture was vortexed for 2 min to obtain a clear suspension. The aqueous phase contained protein and other protein-specific excipients (e.g., trehalose, CaCl$_2$, etc.) used to provide maximum protein stability during SGnP preparation as well as storage at room temperature. The trehalose to protein ratio was varied from 200:1 to 20:1 to increase number of protein molecules in the SGnP (see details the Supporting Information Table S1). The inverse micelle suspension was flash-frozen by spraying it into a 50 mL vial containing liquid nitrogen (N$_2$). The frozen nanoparticles and isooctane in the vial were placed for lyophilization to remove isooctane and water. After lyophilization, the SGnP was washed using isooctane by resuspending and subsequently centrifuging them at 400 to 500*g* for 5 min. The washing process was repeated three times, and finally the SGnP dispersion in isooctane was stored under desiccation at −20 or −80 °C for future use.

2.2.1.2. Fluorescence Dye-Encapsulated SGnP. FITC-tagged BSA and Alexa Flour-tagged BSA were encapsulated into SGnPs following the above-mentioned method.[47] In brief, an aqueous suspension of individual fluorescence dye-tagged BSA, trehalose, and Tween 20 (BSA/trehalose = 1:200) was emulsified in a mixture of AOT in isooctane. The emulsion was flash frozen, followed by sequential removal of the organic and aqueous phase. The final form was washed several times with isooctane, resuspended in isooctane, and stored at −80 °C for future use (See the Supporting Information Table S1 for various protein−SGnP formulations).

2.2.2. Preparation of Protein-Loaded Microspheres. 2.2.2.1. Conventional Emulsion Techniques. Two distinct conventional double emulsion methods, w−o−w and w−o−o were used to prepare protein-loaded microspheres (see the Supporting Information Table S2 for details of the formulations). For preparing microspheres using the w−o−w method

(hereafter named as w−o−w particles), 200 μL of aqueous protein suspension was emulsified in 2 mL of 2.5% (w/v) PLGA in DCM and homogenized at 20 000 rpm for 1 min. The w−o emulsion so formed was further injected by a 22G needle into 50 mL of 2.5% PVA solution followed by homogenization at 12 000 rpm for 5 min. The resultant emulsion was continuously stirred at 500 rpm for 3 h at room temperature for solvent evaporation and particle hardening. The particles were collected by centrifuging at 8000 rpm for 10 min, followed by repeated washing with deionized water. The particles were further lyophilized and stored at 4 °C.

Similarly, for preparing microspheres using the w−o−o method (hereafter named as w−o−o particles), 200 μL of protein in buffer was suspended in 2 mL of 2.5% (w/v) PLGA DCM solution. The suspension was homogenized at 20 000 rpm for 1 min to create the first water−in−oil (w−o) emulsion. The w−o emulsion was injected into 10 mL of paraffin oil (second oil phase). The second emulsion was formed by homogenization at 12 000 rpm for 5 min and then transferred to *n*-hexane for microsphere hardening. The suspension was stirred at 500 rpm for 3 h, followed by centrifugation, and washing with *n*-hexane to remove paraffin oil. The final particles were stored in a vacuum desiccator at 4 °C for future use (see the Supporting Information Table S3 for details of the formulations).

2.2.2.2. Microspheres Incorporating Proteins−SGnP. For preparing SGnP-mediated protein-loaded microspheres, protein−SGnPs were used in place of protein-in-buffer following similar process steps of these two conventional double emulsion techniques, as described above. We prepared two types of protein−SGnP-loaded microparticles using two modified emulsion methods, SGnP-in-oil-in-water (hereafter named as sg−o−w) and SGnP-in-oil-in-oil (hereafter named as sg−o−o) particles. For dual protein-encapsulated (FITC−BSA and Alexa Flour−BSA or FGF-2 and EGF) microparticles, two individual protein-loaded SGnPs were used in a different ratio (w/w). In the SGnP-loaded microparticle preparation, the amount of protein−SGnP was varied from 1.6% (w/w) to maximum 90% (w/w) to achieve theoretical protein loading of 0.008 to 15% (weight of protein with respect to polymer), respectively (see the Supporting Information Tables S4 and S5 for details of the formulations).

2.2.3. Characterization of Nanoparticles and Microparticles. 2.2.3.1. Characterization of SGnPs. The morphology and size distribution of SGnPs were analyzed by cryogenic temperature scanning electron microscopy (Cryo-SEM) (JEOL JSM-7600F). Cryo-SEM imaging was used to image the moisture-sensitive SGnP system. The high vacuum conditions of a usual electron microscope can result in the loss of volatiles from the samples. The Cryo-SEM utilizes low-temperature conditions to reduce vapor pressure to non-considerable values. Cryo-SEM imaging is a valuable technique to efficiently image nanostructures such as our SGnPs.[49] For sample preparation for Cryo-SEM, 10 μL of suitably diluted samples were pipetted out on a carbon tape-coated sample holder. The sample holder was then transferred into the Cryo unit (PP3000T) by Quorum. The cryo preparation chamber was turbomolecular pumped and included tools for cold fracturing, controlled sublimation, and specimen coating. The samples were rapidly frozen in liquid nitrogen (−190 °C) for 30 s under vacuum. Immediately, the samples were subjected to controlled sublimation at −85 °C for 10 min and sputter-coated with platinum at 10 mA for 45 s under vacuum. Then,

the samples were transferred onto a highly stable SEM (JEOL JSM-7600F) cold stage for observation. Cold trapping in the cryo preparation chamber and SEM chamber ensured that the whole process was frost-free. The samples were analyzed in the SEM at an accelerating voltage of 5 keV.

2.2.3.2. Characterization of Microparticles. Microparticle morphology was studied by SEM (Zeiss EVO18). For sample preparation, a dilute suspension of each microsphere was dropped onto carbon tapes on aluminum stubs, allowed to air dry, and sputter coated with gold−palladium. The particle size was estimated from SEM micrographs using ImageJ (NIH software) considering 150 particles for each sample.

2.2.4. Protein Distribution Study into the Microparticle Matrix Using Confocal Microscopy. Confocal laser scanning microscopy (Leica TCS SP8) was used to visualize the distribution of the protein (single and dual proteins) in the microparticle polymer matrix. Two fluorescence proteins, FITC−BSA and Alexa Flour−BSA, were encapsulated into the microparticles. Microparticles loaded with a single protein (FITC−BSA) as well as dual proteins (both FITC−BSA and Alexa Flour−BSA) were prepared by the conventional (protein-in-buffer) and protein-in-SGnP-mediated emulsion methods. We used an excitation/emission wavelength of 495 nm/519 nm and 652 nm/670 nm to visualize the FITC−BSA and Alexa Flour−BSA in the microparticles, respectively.

2.2.5. Quantification of Proteins. Three protein assay kits, namely Micro BCA, NanoOrange, and ELISA (FGF-2 and EGF), having a difference in detection limits were used to quantify the protein in particles and release medium according to the manufacturer's protocol.

2.2.5.1. Micro BCA Protein Assay. This assay was used to estimate BSA and HRP extracted from the microparticles or released from microparticles. In brief, model proteins (BSA and HRP) were diluted in a suitable buffer [1× phosphate-buffered saline (PBS), pH 7.4 for BSA and 50 mM TRIS, pH 5.5 for HRP] and added in triplicate in 96-well plates followed by addition of BCA working reagent. The plates were incubated at 37 °C for 2 h. Absorbance reading was taken at 562 nm in a microplate reader (PerkinElmer). The amount of total protein was determined from the standard curves of BSA and HRP using micro BCA assay (see the Supporting Information Figure S1a,b).

2.2.5.2. NanoOrange Protein Quantification. The total amount (ELISA active and inactive part) of growth factor (FGF-2/EGF) was quantified using the NanoOrange protein quantification kit. In brief, the release samples of FGF-2/EGF from microparticles at specific intervals were aliquoted. The samples were diluted in light-sensitive 1× NanoOrange working solution. The diluted samples were incubated at 90 to 96 °C for 10 min in the dark. The fluorescence reading was recorded at 470 nm/570 nm excitation/emission wavelength using a plate reader (PerkinElmer). The concentrations of the released FGF-2/EGF were determined from the standard curve (see the Supporting Information Figure S1d).

2.2.5.3. ELISA. Sandwich ELISA was used to quantify the amount of active (capable of binding to antibody) FGF-2 and EGF released from microparticles at specific intervals according to the manufacturer's protocol. In brief, the plate was developed using anti-FGF-2/EGF primary antibody (capture antibody) and blocking buffer. Standard FGF-2/EGF (100 μL) and release aliquots of FGF-2/EGF samples were added in triplicate to each well of developed plate, followed by the addition of biotinylated FGF-2/EGF

secondary antibody (detection antibody) and Avidin−HRP conjugate to each well. Finally, 100 μL of ABTS liquid substrate was added to each well and absorbance was read at 405 nm every 5 min until 25 min in a microplate reader (PerkinElmer). The concentration of the samples was calculated from the standard FGF-2/EGF plot (see the Supporting Information Figure S1e,f).

2.2.6. Encapsulation Efficiency and Loading Capacity. The protein encapsulation efficiency was estimated following a previously published protocol with slight modifications.[50] In brief, 10 mg of dried microspheres were dissolved in 1 mL of DCM followed by the addition of 2 mL of PBS. The vials were shaken overnight to extract the protein into the aqueous phase. Respective protein quantification assay was performed to determine the encapsulation efficiency and loading capacity of the microparticles using the following equations. Theoretical loading denotes the amount of protein loading set to achieve theoretically with respect to weight of the polymer matrix of microparticles. The following equations were used to calculate encapsulation efficiency and loading capacity

$$
\text{Encapsulation efficiency} = \frac{\text{weight of encapsulated protein}}{\text{weight of total protein used for encapsulation}} \times 100\%
$$

$$
\text{Loading capacity} = \frac{\text{weight of encapsulated protein}}{\text{weight of microparticles}} \times 100\%
$$

2.2.7. In Vitro Release Assay for Proteins. 2.2.7.1. Release of BSA. Model protein BSA was used to study the release kinetics of BSA from different microparticles (w−o−w, sg−o−w, w−o−o, and sg−o−o). In brief, 10−15 mg of dried microspheres were placed in 1 mL of 1× PBS (pH 7.4) in 1.5 mL microcentrifuge tubes in triplicate. The vials were maintained at 37 °C in a shaker incubator rotating at 50 rpm speed for four weeks. At predetermined intervals (up to 30 days), 1 mL released medium was collected and replaced by fresh medium. Micro BCA protein assay was performed to determine the amount of released protein.

2.2.7.2. Release of FGF-2/EGF. The release kinetics of active FGF-2/EGF from the different w−o−w and sg−o−w microparticles were determined using ELISA. In brief, 20 mg of dried microspheres were placed in 1.5 mL microcentrifuge tubes in triplicate and suspended in 1 mL of 1× PBS (pH 7.2). The vials were maintained at 37 °C in a shaker incubator rotating at 50 rpm speed for release studies. At predetermined intervals (up to 10 days), the microparticles were collected by centrifugation at 5000 rpm for 5 min. The entire supernatant was assayed for protein release and replaced by 1 mL of fresh release medium. ELISA was performed to determine the amount of active FGF-2/EGF fraction in the released protein as described before.

To study the bioactivity of FGF-2 released at specific intervals from particles, the release experiment was performed in a sterile environment. In brief, 10−15 mg of GF-loaded (FGF-2) particles were placed in 24-well plates and sterilized with ethanol (70%) for 5 min, followed by removal of ethanol and washing with 1× PBS three times. The particles were then sterilized using UV for 30 min, followed by the addition of 1 mL of 1× PBS for release studies. The plate was placed on a
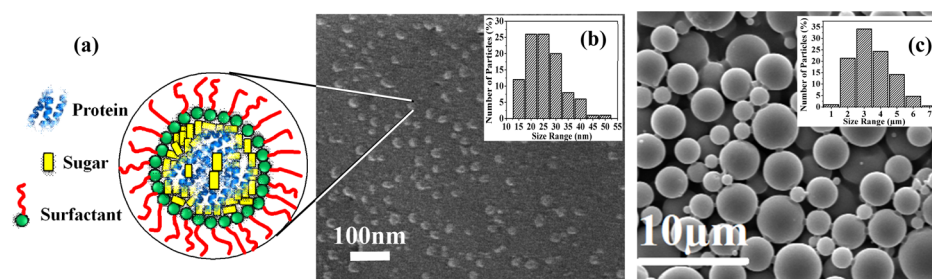
Figure 1. Morphology and size distribution of protein-loaded SGnP and protein-loaded PLGA microparticle. (a) Schematic representation of the design of a protein−SGnP system. (b) Cryo-SEM image of BSA−SGnPs and their size distribution (inset). 1:200 (BSA/trehalose) was used to prepare the BSA−SGnPs nanoparticles. (c) SEM image of BSA−SGnP-loaded (1% theoretical BSA loading) PLGA microparticles (sg−o−w) and their size distribution (inset).

gyratory shaker rotating at 25 rpm inside the sterile incubator maintained at 37 °C. At predetermined intervals (1, 3, and 7 days), the entire release medium from each well was collected and replaced by fresh PBS.

2.2.8. Protein Activity Assay. Protein activity loss during the processing of microparticles was probed using three model proteins, HRP, FGF-2, and EGF. We have performed enzyme activity assay for HRP protein. Antibody binding activity and cell-based bioactivity assay were performed to probe the activity of FGF-2 and EGF. Protein activity loss during storage was studied using HRP as a model protein.

2.2.8.1. Enzymatic Assay for HRP. The residual activity of HRP in the microparticles, as well as released media, were evaluated using *o*-phenylenediamine (OPD)-based HRP enzymatic assay, as described in the literature.[51] HRP catalyzes the oxidative coupling reaction of OPD to 2,3-diaminophenazine, which was measured by colorimetry at 430 nm. The HRP sample (0.050 mL) was added to 0.150 mL of substrate solution in each well of 96-well plates to initiate the reaction. After incubation for 30 min at room temperature (25 °C), the absorbance of samples was recorded at 430 nm. The absorbance of substrate solution at 430 nm was used as blank correction (see the Supporting Information Figure S1c). NanoOrange assay was performed to determine total protein (enzymatic active and inactive component). The percentage of active protein was determined using a standard plot of HRP and expressed with respect to the total protein (see the Supporting Information Figure S1d).

2.2.8.2. Antibody-Binding Activity of FGF-2/EGF by ELISA. The ELISA active fraction of FGF-2 and EGF (antibody binding activity) was determined by ELISA. The total protein was determined by the NanoOrange protein assay. The percentage of active protein was determined and expressed with respect to the total protein (see the Supporting Information Figure S1e,f).

2.2.8.3. Bioactivity of FGF-2 Using HGF. The bioactivity of FGF-2 was studied by checking dose-dependent proliferation of HGF. The cells were grown in Dulbecco's modified Eagle's medium (DMEM) with 10% fetal bovine serum (FBS) and 1% pen−strep (Invitrogen). In brief, HGF cells were seeded at a density of 3000 cells/well in 96-well plates and cultured with 10% FBS DMEM, for 24 h. The media was then replaced with serum-free DMEM supplemented with different concentrations of FGF-2 (0 to 10 ng/mL) and/or known concentration (measured by NanoOrange method and ELISA) of released FGF-2 (at 24 h) from different particles. Only DMEM media and reconstituted GF of concentration similar to released FGF-2 were used as a negative and positive control for cell

proliferation assay. The cell viability of HGF was analyzed after 48 h of incubation with FGF-2 using the calorimetric 3-(4,5-dimethylthiazol-2-yl)-5-(3-carboxymethoxyphenyl)-2-(4-sulphophenyl)-2*H*-tetrazolium (MTS) assay (Promega). Cells were washed with PBS and incubated with 20% MTS reagent in serum-free medium. After 4 h of incubation at 37 °C in 5% CO_2 incubator, supernatant of all wells were collected, and absorbance was measured at 490 nm using a microplate reader (PerkinElmer). After MTS, the cell densities in different wells were imaged using optical microscopy.

2.2.9. Protein Storage Stability Study. HRP was used as a model protein in the storage stability study of encapsulated protein in the different microparticles (w−o−w, w−o−o, sg−o−w, and sg−o−o). HRP-loaded microspheres were stored at three different temperatures namely, −80, 4, and 25 °C for over 100 days. At predetermined intervals of 7, 14, 30, 60, 75, and 100 days, the microparticles were removed from storage, and the residual activity of the entrapped HRP was quantified after extracting the total protein from the microsphere following the procedure explained earlier.

2.2.10. Ex Vivo Functional Assay of Protein Depot. We used the "cancer stem cell mammosphere formation" assay as a model ex vivo functional assay for dual protein-loaded (FGF-2 and EGF) protein depot. Human breast carcinoma cell line (MCF7) cells were used for this assay.

2.2.10.1. Cancer Stem Cell Mammosphere Formation. Cells were cultured in DMEM (High Glucose, HIMEDIA) supplemented with 10% FBS (HIMEDIA) and maintained under 5% CO_2 in a humidified atmosphere at 37 °C. For "cancer stem cell mammosphere formation", cells were seeded at a cell density of 10 000 cells/well in 24-well ultralow attachment plates (Corning, Sigma) in serum-free DMEM-F12 media (Himedia) supplemented with 1× B27 and incubated at 37 °C, supplied with 5% CO_2. Cells were seeded as two groups in duplicate. The first group was cultured with a regular supplement of free growth factors and the second cultured in the presence of 10 mg of dual protein-loaded (EGF and bFGF) sg−o−w microparticles suspended in trans-well inserts containing 500 μL DMEM-F12 media. The sphere cultures were maintained for 7 days with media change done every 3 days. The different GF (FGF-2 and EGF) concentration in the media was measured at 3 and 7 days using ELISA. The number of spheres formed was counted under a microscope and used for further analysis. Transformation efficiency was calculated using the following formula
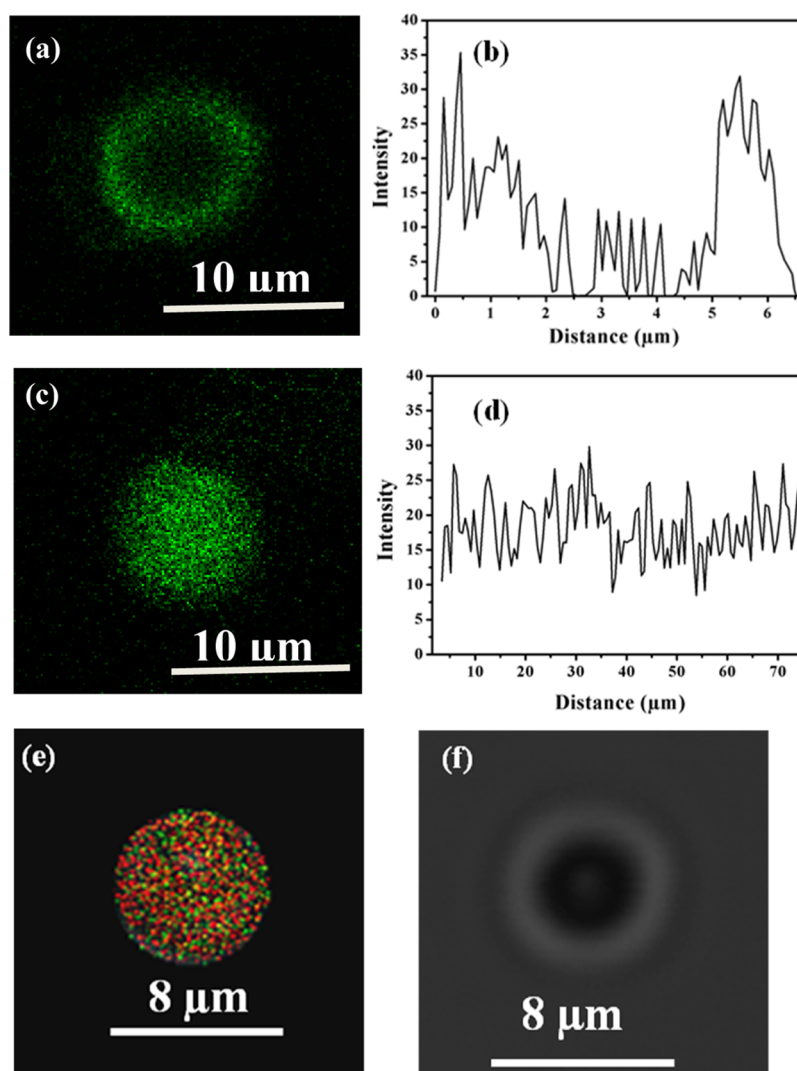
Figure 2. Protein distribution within the microparticle polymer matrix by confocal microscopy (a) FITC−BSA distribution within the particles prepared by the conventional emulsion technique (w−o−w), and (b) fluorescence intensity plot along the particle diameter showing preferential distribution of protein along periphery of the particle. (c) FITC−BSA distribution in particles prepared by our SGnP-mediated emulsion technique (sg−o−w), and (d) fluorescence intensity distribution along particle diameter showing uniform distribution of protein throughout the particle. (e) Dual proteins (FITC−BSA and Alexa Flour−BSA) in a single microparticle system encapsulated using our SGnP system, showing distinct and uniform distribution of individual protein throughout the particle matrix, and (f) representative bright field image of green dye-BSA−SGnP-loaded PLGA microparticle.

% Tranformation efficiency

$$= \frac{\text{no. of spheres formed}}{\text{total no. of cells seeded}} \times 100$$

2.2.10.2. Flow Cytometry Analysis. Monolayer cells (MCF7), as well as the mammospheres, were dissociated using Accutase 1× (HIMEDIA) into single cell suspensions. After washing with 1× PBS, 1×10^6 cells were resuspended in FACS buffer (1× PBS-1% BSA, Sigma, USA) containing Alexa Fluor 647-conjugated CD24 antibody (BioLegend) and incubated for 30 min on ice. As negative controls for flow cytometry analysis, we used isotype-matched conjugated nonimmune antibodies. Nonspecific antibody binding was removed by washing two times with 2% BSA-1× PBS and analyzed on a flow cytometer (BD FACS Aria III) using FACSDiva Software.

2.2.11. Statistical Methods. The data were expressed as mean ± standard deviation. One-way analysis of variance (ANOVA) was employed to assess statistical significance using GraphPad InStat software package.

3. RESULTS

3.1. Nanoparticles/Microparticle Morphology and Size Distribution. Dye or protein-loaded SGnPs were prepared by slightly modifying our previously developed method.[47] Particle morphology and size distribution of the BSA-loaded SGnP and BSA−SGnP-loaded PLGA-microparticles are shown in Figure 1. The design of the sugar-glass nanoparticle system is represented in Figure 1a. Protein molecules (>10 numbers) are sequestrated into the glassy matrix of sugar (with other excipient), stabilizing the protein molecules from process- and storage-related stresses. Furthermore, the surfactant (AOT) on the particle surface provides excellent dispersion properties of the particles in organic solvent−polymer solution. Cryo-SEM image of BSA−SGnP (Figure 1b) shows monodispersed spherical particles

Table 1. Summary of the Encapsulation Efficiency and Loading Capacity of BSA in PLGA Microparticles[a]

protein	theoretical loading (%)	emulsion method	encapsulation efficiency (%)	loading capacity	release at 24th h (%)
BSA	0.008	w−o−w	87 ± 0.91	0.003 ± 0.12	69.3 ± 0.13
		sg−o−w	98 ± 4.62	0.006 ± 0.36	8.5 ± 0.09
	0.01	w−o−w	90.1 ± 2.71	0.007 ± 0.15	73.98 ± 2.82
		sg−o−w	95.6 ± 2.16	0.008 ± 0.42	10.19 ± 2.85
	0.05	w−o−w	78 ± 1.53	0.03 ± 0.34	54.9 ± 3.36
		sg−o−w	92 ± 0.56	0.045 ± 0.23	5.6 ± 1.57
	1	w−o−w	52 ± 0.33	0.5 ± 0.02	61 ± 2.18
		sg−o−w	90 ± 0.17	0.9 ± 0.12	21.2 ± 5.91
	5	w−o−w	42 ± 0.03	2.1 ± 0.01	43.3 ± 2.44
		sg−o−w	64 ± 0.15	3.25 ± 0.16	14.6 ± 3.71
HRP	0.1	w−o−w	69 ± 0.63	0.05 ± 1.25	52.76 ± 0.34
		sg−o−w	88.7 ± 0.61	0.09 ± 0.67	10.45 ± 1.45
FGF-2	0.01	w−o−w	79 ± 0.98	0.0045 ± 0.45	32.6 ± 2.56
		sg−o−w	96 ± 0.24	0.008 ± 0.78	7.8 ± 2.92
EGF	0.01	w−o−w	82 ± 0.56	0.005 ± 0.43	32.5 ± 4.27
		sg−o−w	99.76 ± 3.73	0.009 ± 0.93	10.25 ± 2.74
FGF-2 & EGF	0.01	w−o−w	64 ± 2.64	0.005 ± 0.17	49.4 ± 1.69
		sg−o−w	91.23 ± 0.65	0.007 ± 0.34	10.7 ± 2.2

[a]Abbreviations: w−o−w: water-in-oil-in-water, sg−o−w: sugar glass-in-oil-in-water. The data represents average of three independent readings ± standard deviation.

with an average size of 23 ± 0.5 nm. Note that we have used 1:200 (BSA/trehalose) to prepare the BSA−SGnPs nanoparticles. When the trehalose/BSA amount is reduced to 20:1, agglomerated BSA−SGnP was obtained (see Figure S2 for the Cryo-SEM imaging). However, all SGnP formulation used in this study with variable trehalose to protein ratio (see Table S1) was found to have average particle size between 23 and 30 nm, except the lowest trehalose formulation (trehalose/BSA = 20:1) SGnP (50 to 100 nm). The surface morphology of the SGnP-loaded (1% theoretical BSA) PLGA microparticles prepared by sg−o−w emulsion (Figure 1c) reveals that they are nonporous spherical particles of average size 3 ± 0.85 μm. All other microparticles prepared by different methods are observed to have similar size distribution (see the Supporting Information Figure S3).

3.2. Protein Distribution in the Microparticle Matrix Using Confocal Microscopy. To study the distribution of protein in the polymer microparticles matrix, two fluorescence proteins, FITC−BSA and Alexa Flour−BSA were used as the model protein systems and encapsulated individually/in combination into the microparticles using conventional emulsion as well as our SGnP-mediated emulsion methods (Figure 2). Figure 2a,b shows the protein distribution and fluorescence intensity plot in the microparticle prepared by the conventional emulsion (w−o−w) method. Proteins are observed to be not uniformly distributed throughout the polymer matrix but preferentially distributed toward the periphery of the w−o−w microparticle. This is further supported by the fluorescence intensity along the diameter of the particle plot (Figure 2b). A similar distribution of protein was observed in the w−o−o microparticle (see the Supporting Information Figure S4a). On the other hand, our protein−SGnP-mediated encapsulation (sg−o−w) results in uniform distribution of protein throughout the polymer matrix as nanosized particles (without any clump of protein) confirmed by confocal image and fluorescence intensity plot (Figure 2c,d). We observed similar nanosized protein distribution in sg−o−o microparticles (see the Supporting Information Figure S4b). Figure 2e depicts distribution of dual proteins in a single

microparticle system encapsulated using our green dye-BSA−SGnP and red dye-BSA−SGnP-systems and prepared by the sg−o−w method. It shows uniform distribution of both proteins throughout the polymer microparticle matrix. Moreover, it is clear that the individual proteins are distinctly separated and protected within the SGnP matrix. Figure 2f shows a representative optical microscopy image of the green dye-BSA−SGnP-loaded microparticle (sg−o−w).

3.3. Protein-Loading Capacity and Encapsulation Efficiency. Loading capacity and encapsulation efficiency of different model proteins encapsulated by different methods (w−o−w and sg−o−w) are represented in Table 1. Note that all data related for w−o−o and sg−o−o particles are presented in the Supporting Information (see the Supporting Information Table S6). The encapsulation efficiency and loading capacity were determined for different microparticle systems prepared by the w−o−w and sg−o−w methods with variable theoretical protein-loading capacity from low (0.008%) to high (5%) using the BSA model protein system. Encapsulation efficiency and loading capacity for different protein-loaded microparticles (Table 1) depend on their theoretical target protein-loading amount. As expected, the encapsulation efficiency gradually decreases with increase in their theoretical target protein-loading capacity, for example, 0.008 to 5 (%). BSA encapsulation efficiency for sg−o−w is 98% for 0.008% theoretical protein loading, and 64% for 5% theoretical protein loading. Similarly, the SGnP-mediated sg−o−o method results in 93% encapsulation efficiency for 1% theoretical loading and 70% for 5% theoretical loading (see the Supporting Information Table S6). However, for any microparticle sample with specific target protein loading, particles prepared by sg−o−w/sg−o−o show higher encapsulation efficiency and loading capacity compared to particles prepared by the conventional w−o−w/w−o−o method. As an example, encapsulation efficiency of BSA is 52 and 90% for particles prepared by w−o−w and sg−o−w, respectively, with the theoretical target protein loading of 1%. Similarly, loading capacity (BSA) of 0.5 and 0.9% were achieved in the particles
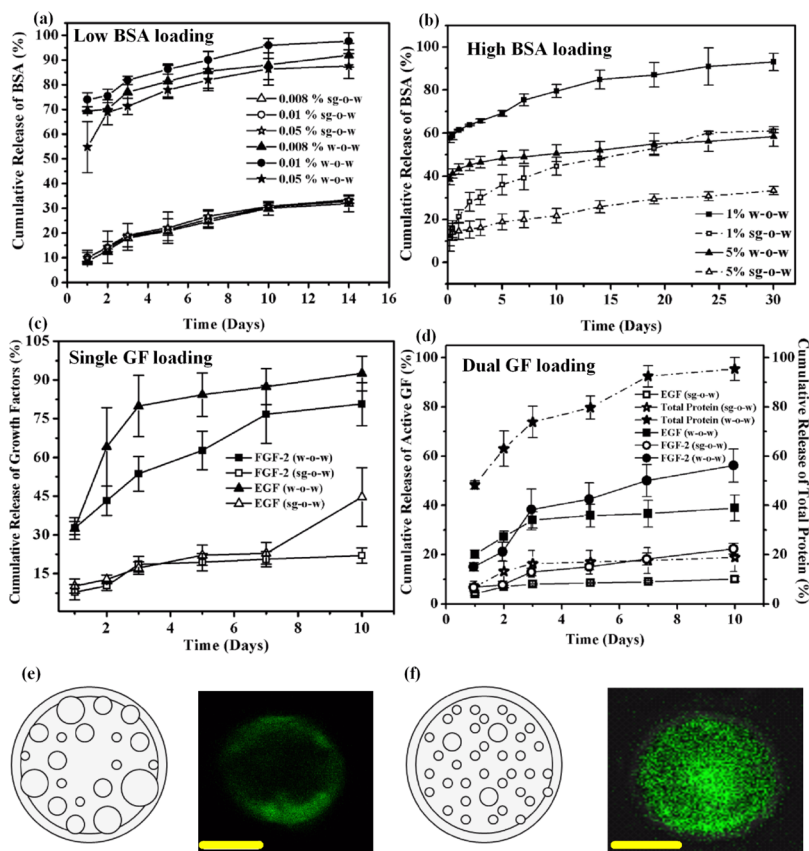
Figure 3. Release profiles of model proteins. Cumulative release of BSA from different amount of protein-loaded PLGA microparticles prepared by the w−o−w and sg−o−w methods (a) with low theoretical BSA loading, 0.008% (w/w) to 0.05% (w/w) to polymer matrix and (b) with high theoretical BSA loading, 1% (w/w) and 5% (w/w) to polymer matrix. (c) Cumulative release of total FGF-2 and total EGF from PLGA microparticles prepared by the conventional w−o−w and our sg−o−w method with theoretical loading of protein 0.01% (w/w) of polymer matrix measured by the NanoOrange method. (d) Dual cumulative release of FGF-2 and EGF from PLGA microparticles prepared by the sg−o−w and w−o−w methods with theoretical loading of protein 0.01% (w/w) of polymer matrix. Cumulative release of active fraction was determined by ELISA (antibody binding active fraction) as well as total protein (active + inactive) measured by the NanoOrange method. Schematic representation of protein distribution in the microparticle matrix prepared by (e) conventional w−o−w method and (f) prepared by SGnP-mediated sg−o−w method. Insert is respective confocal image showing actual protein distribution. The scale bar in (e) and (f) is equal to 10 μm.

prepared by the w−o−w and sg−o−w methods, respectively, with a target theoretical loading capacity of 1%.

3.4. Release Profile of Single and Multiple Proteins. Figure 3 represents release profiles of model proteins from w−o−w and sg−o−w microparticles (the amount of protein released within the first 24 h is represented in Table 1). The release profiles of all protein-loaded formulations is divided into two categories based on the amount of protein loading; low protein-loading (0.008 to 0.05%) microparticles and high protein-loading microparticles (1 to 5%). Figure 3a represents the release profile of BSA from microparticles prepared by the conventional w−o−w and our SGnP-mediated sg−o−w emulsion methods with low theoretical protein loading, 0.008 to 0.05% (w/w). The release profiles of BSA from low protein-loaded particles show high burst release (55−74%) for particles prepared by the conventional w−o−w method compared to only 5−8% release from particles prepared by our sg−o−w method. Moreover, for low target BSA-loaded particles, almost 100% release of BSA was observed at day 14 from the w−o−w particles compared to only ∼30% release from sg−o−w particles. Figure 3b accounts for the release profile of BSA from microparticles with high target theoretical protein loading (1 and 5%) prepared by w−o−w and sg−o−w. Release profiles of microparticles prepared by the w−o−w

method show very high release within 24 h (burst release) followed by sustained release of protein. 61 and 43% of protein release occurs within 24 h from 1 to 5% protein-loaded w−o−w microparticles, respectively (Table 1). Similar release profiles are also observed for w−o−o microparticles, 76 and 81% for 1 and 5% theoretical protein loading, respectively (see the Supporting Information Figure S5). On the other hand, only 21 and 15% of protein release is observed from 1 to 5% theoretical protein-loaded sg−o−w microparticles, respectively. Release profiles of two model GFs, EGF and FGF-2, from two types of particles are similar to low-BSA-loaded microparticles. Note that NanoOrange was used to estimate the total GF (active and inactive fraction) in the release media. The initial release of FGF-2/EGF from w−o−w microparticles is ∼33% compared to only 7 to 10% for sg−o−w particles, which is 3.5- to 5-fold higher than that for the sg−o−w particles (Figure 3c). Figure 3d shows the release profile of dual GFs (EGF and FGF-2) from particles prepared by the w−o−w and sg−o−w methods, where GFs were quantified using two methods, such as NanoOrange for total release GF in the media (total GF including ELISA active and inactive fraction of both GF, EGF and FGF-2) and ELISA (specific to GF, EGF, or FGF-2) for active fraction of specific GF in the release medium. The release profiles of active fractions of individual
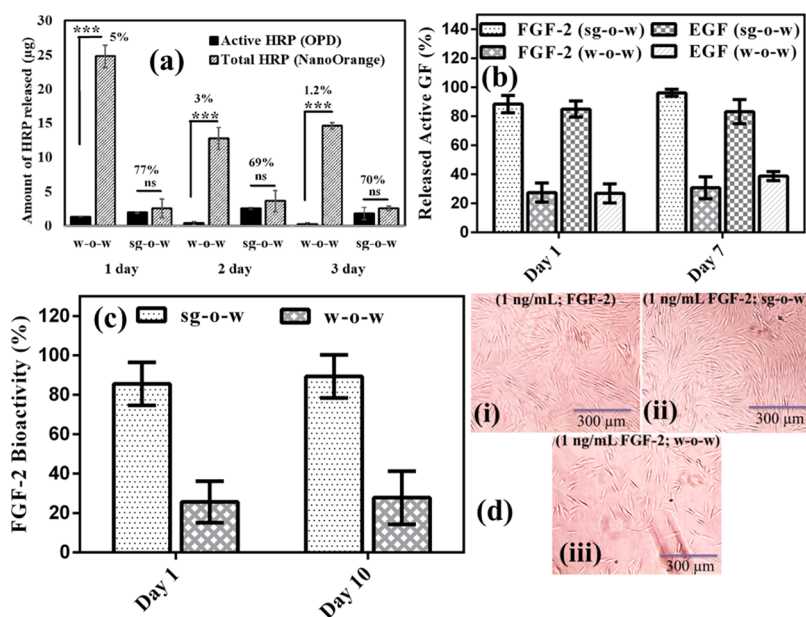
Figure 4. Protein activity preservation during processing of microparticles. (a) Amount of active and total HRP released from w−o−w and sg−o−w microparticles at day 1, 2, and 3. (b) Percentage of ELISA active FGF-2 and EGF in the released fraction (day 1 and 7) from different microparticles, w−o−w, and sg−o−w particles. (c) Percentage of bioactive FGF-2 in the released fraction (day 1 and 10) from two different microparticles (w−o−w, and sg−o−w) measured by proliferation assay of HGF cells. (d) Representative picture of HGF cell density and morphology in different treated samples, (i) positive control, 1 ng/mL FGF-2 supplemented, (ii) 1 ng/mL FGF-2 eluted from sg−o−w, and (iii) 1 ng/mL FGF-2 eluted from w−o−w sample. Total FGF-2 used for HGF proliferation was quantified using NanoOrange. The data for comparisons between conventional and our system are shown to be very significant where the **$P < 0.01$.

protein (EGF or FGF-2) from a particular type of particle, w−o−w or sg−o−w, measured by ELISA (determining the antibody binding active fraction) show burst-free sustained release (∼7%) for sg−o−w particles and (15−20%) w−o−w particles. However, percent (%) of total protein (ELISA active fraction plus inactive fraction of both GFs) released (measured by NanoOrange) from the particles (w−o−w or sg−o−w) shows a release profile similar to their individual protein (BSA, FGF-2, and EGF) release from their respective particles system as depicted in Figure 3a,c, that is, high burst release (∼49%) from w−o−w microparticle and only ∼6% release from sg−o−w particles. Please see the Supporting Information Table S8 for raw data and calculation of active fraction and total protein (active and inactive fraction).

3.5. Preservation of Protein Activity during Preparation of Microparticles. To determine the preservation capacities of our SGnP system in the microemulsion method, we have comparatively evaluated the protein (HRP, FGF-2, and EGF) activity loss during preparation of microparticles by the conventional (w−o−w) as well as SGnP-mediated emulsion methods (sg−o−w). The activity loss of different proteins such as HRP and GFs during processing of microparticles was checked by measuring the amount of active fraction (enzymatic active fraction for HRP, ELISA-active fraction of EGF or FGF-2, and bioactive fraction of EGF or FGF-2) in the total released protein from the different types of microparticles, depicted in Figure 4. Figure 4a shows the amount of active and inactive HRP present in the released medium. In the day 1 released fraction, 95% HRP (23.55 μg inactive out of 24.8 μg) are in inactive form for w−o−w particles compared to only 24% (0.61 μg inactive out of 2.5 μg) inactive HRP for sg−o−w particles. Active fraction of HRP in the other released samples (at day 2 and 3) have the similar trend, that is, 99% (14.43 μg inactive out of 14.6 μg) HRP are

in inactive form in the day 3 released medium from w−o−w particles, in contrast to only 30% (0.74 μg inactive out of 2.5 μg) inactive fraction of HRP in the released medium from sg−o−w particles. Note that the active HRP fraction in the day 7 or day 10 released medium could not be estimated, as HRP was found to lose its activity during incubation in the release medium for longer than 3 days at room temperature. The activity loss (antibody binding activity) of GF (FGF-2 and EGF) during processing of microparticles was also checked by measuring the ELISA-active fraction in the total released protein from the different types of microparticles, depicted in Figure 4b. More than 85% FGF-2/EGF (GF) are active in all release samples from sg−o−w microparticles compared to less than 30% active GF present in the release samples from w−o−w microparticles. This result shows that more active GFs (>3 fold) are in all of the release samples (day 1 and day 7) from sg−o−w microparticles than conventional w−o−w microparticles. Similarly, HGF cells were used to measured bioactivity (FGF-2-induced cell proliferation) of released FGF-2 from different particles (w−o−w and sg−o−w) (see the Supporting Information Figure S6, FGF-2 dose-dependent proliferation of HGF cells). Figure 4c shows the amount of biologically active GF (measured by cell proliferation) fraction in the released GF from the two different microparticles where NanoOrange was used to quantify the total protein (active and inactive fraction) presence in the eluted media. The FGF-2 released (at day 1 and day 10) from the sg−o−w microparticles has >85% biologically active fraction compared to only <25% active fraction from w−o−w particles (Figure 4c,d). Figure 4d shows the cellular morphology and density in the culture wells treated with different eluted (day 1) FGF-2 samples (1 ng/mL of total GF including active and inactive fraction). The cell density is in agreement with the ELISA active fraction present in the different eluted FGF-2 samples at
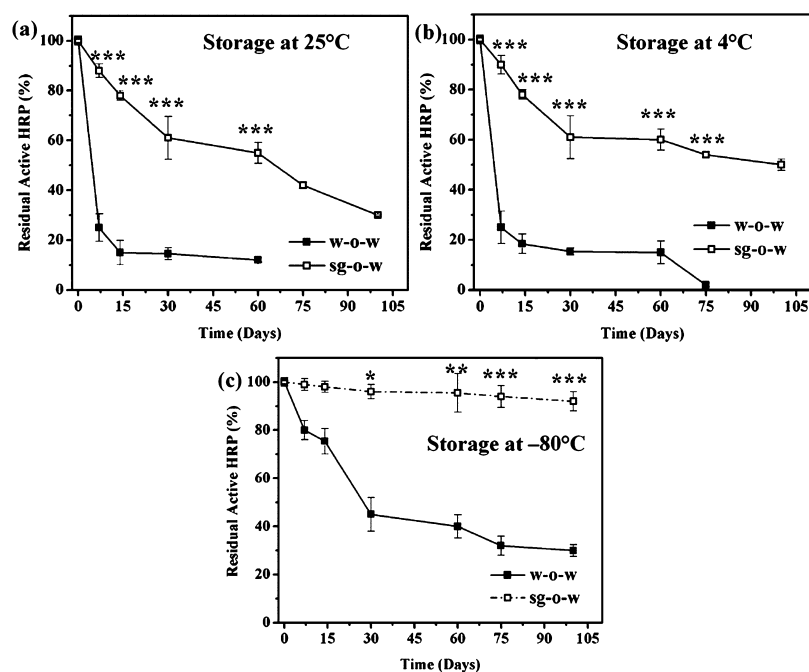
Figure 5. Three months storage stability of HRP in different microparticles (w−o−w and sg−o−w) after storage at three different temperature points. Residual active HRP in the different microparticles, (a) stored at 25 °C, (b) stored at 4 °C, and (c) stored at −80 °C. Residual HRP activity at each time point is compared for significance between conventional and sugar-glass-incorporated systems. Results indicate that SGnP incorporation data is extremely significant (***$P < 0.001$) at majority of the study points. Here, ***$P < 0.001$, **$P < 0.01$, *$P < 0.05$.
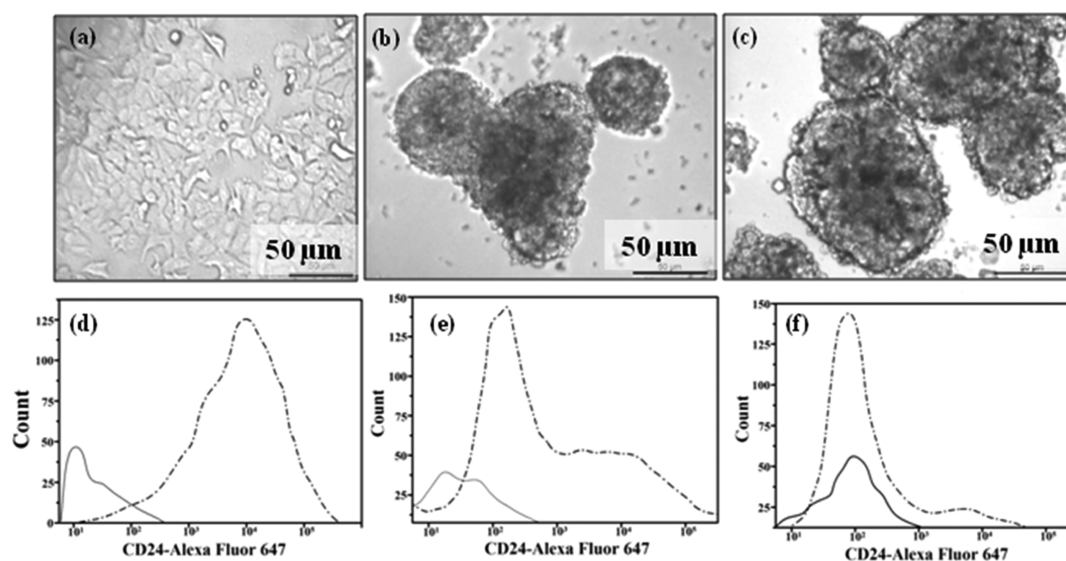

Figure 6. Cancer stem cell mammosphere formation and their CD24 status, after 7-days culture under different conditions. (a−c) shows the morphology of (a) MCF 7 cell line, (b) mammosphere culture with regular addition of FGF-2 + EGF, and (c) mammosphere culture in the presence of FGF-2 + EGF-loaded protein depot. The image scale is 50 μm. (d−f) represents expression of CD24 in (d) MCF-7 cell line, (e) MCF-7 mammospheres generated with regular replenishment of FGF-2 + EGF, and (f) MCF-7 mammospheres generated in the presence of FGF + EGF-loaded protein depot. The solid line in (d−f) represents unstained cells, and the dotted line represents cells stained with Alexa Flour 647-tagged CD24 antibody.

day 1 (Figure 4c). Antibody binding active fraction (ELISA active) of FGF-2 in the eluted samples (at day 1 and day 10) from two types of microspheres are ∼90% in sg−o−w and ∼25% in w−o−w samples, similar to their respective bioactive fraction (Figure 4c), that is, more than 3-fold active FGF-2 in our sg−o−w particles than in the conventional w−o−w particles. ELISA activity and bioactivity of FGF-2 in the respective eluted samples exhibit >3 times more activity of FGF-2 when protected by SGnP.

3.6. Preservation of Protein Activity during Storage of Microparticles.
To determine the storage stability of the protein in the microparticles prepared by different methods, we quantified the residual active HRP in microparticles during storage at three different temperatures, −80, 4, and 25 °C for 100 days. Figure 5 shows the residual activity (%) of the protein (HRP) in various microparticles (w−o−w and sg−o−w) during storage at three different storage temperatures. The activity of HRP in the microparticles prepared by conventional

emulsion methods, w−o−w and w−o−o (for w−o−o emulsion results, see the Supporting Information Figure S7) decay very fast to zero on 50th day of storage at both temperatures, 4 and 25 °C. On the other hand, activity of HRP in microparticles when protected by the SGnP system (sg−o−w and sg−o−o) decay very slowly, and over 50% protein remains active after 100 days of storage at 4 and 25 °C. Even when stored at −80 °C, the unprotected HRP in the microparticle (w−o−w and w−o−o) gradually decays to <40% activity after 80 days, compared to almost zero activity decay of HRP (100% activity) in SGnP-protected microparticles (sg−o−w and sg−o−o).

3.7. Ex Vivo Functional Assay of Protein Depot. Finally, we used dual protein-loaded microparticles (FGF-2 and EGF) for "cancer stem cells (CSCs) mammosphere formation" as a model ex vivo functional assay for protein depot that mimics in vivo protein release and their function. Figure 6 represents the formation of mammospheres as well as differential expression of the stem cell marker, CD24, in the presence and absence of the protein depot. As shown in Figure 6b,c, the number of spheres formed is found to be similar in both the groups with transformation efficiency values, 2.09 ± 0.12 and 1.92 ± 0.03, respectively, for those generated in the presence of free growth factors and in the presence of growth factor-loaded protein depot. Upon analysis of the stem cell marker, CD24, majority of the mammosphere cells generated in the presence of free growth factors as well as the protein depot show significant decrease in the expression of CD24 as compared to the MCF-7 cell line. However, mammospheres developed in the presence of the protein depot exhibit a further increase of cell population, which has decreased expression of CD24 compared to those generated in presence of free growth factors (Figure 6d−f).

4. DISCUSSION

A sustained-release, injectable, polymer microparticle-based therapeutic protein depot has immense clinical importance in drug delivery and tissue engineering, as this improves patient compliance and efficacy and makes protein therapy cost effective.[2,10,43] However, the common emulsion-based methods for the preparation of microparticle protein depots have been facing several protein delivery challenges such as low encapsulation efficiency, uncontrolled release, and activity losses during processing and storage.[10] These critical barriers resulted in limited success of protein depots in clinic; the best-known example is Nutropin Depot, a sustained delivery system of hGH. To overcome these challenges, we have developed a generic protein-nanoencapsulation (SGnP)-mediated emulsion method for the preparation of polymer microparticle protein depot.

The sugar-glass-incorporated microparticles results in a spherical structure of average size 3 ± 0.85 μm. Note that incorporation of the protein−SGnP in the microparticle system renders no change in the size distribution and surface morphology of the PLGA microparticles. As we reported earlier, the [water]/[surfactant] mole ratio (w = [H$_2$O]/[AOT]) plays a significant role in determining the SGnP size, and similarly, mass ratio of protein to trehalose can be tuned from 1:500 to 1:200 to provide sufficient coating of sugar glass around the protein without adversely affecting performance. One of the major requirements for a protein depot is to maximize the protein-loading capacity into the microparticles to ensure longer delivery of protein. To achieve high protein

loading, first we made different SGnP formulation with the maximum number of protein molecules in each SGnP system. We made a series of BSA-loaded SGnP systems with varying amounts of trehalose for specific amounts of protein to maximize the number of protein molecules in each SGnP matrix without compromising other benefits of the SGnP system such as protection during processing, storage, and so forth. Moreover, in addition to reducing the trehalose amount, we have prepared smaller-size SGnP systems to increase the confinement of protein into smaller nanostructures, which may help to stabilize the protein as well as improve the dispersion of the SGnPs into the polymer matrix.[52] Thus, in this study, smaller size of SGnP (23 ± 0.5 nm) was prepared using the [water]/[surfactant] ratio (mole) of 10. Similarly, to maximize protein encapsulation per SGnP (>10 proteins), protein to trehalose ratios (mass ratio) from 1:20 to 1:200 were used. We observed that the trehalose to protein ratio could be reduced up to 20:1 without significant effect on protein stabilization when the SGnP size was reduced to 23 nm. However, we found significant agglomeration of SGnP, particularly in the lowest trehalose/BSA (protein) ratio, that is, 20:1 (see the Supporting Information Figure S2). Thus, the mass ratio of protein/trehalose of 1:20 for BSA encapsulation was used to maximize protein loading into SGnP at the expense of agglomeration of SGnPs in the suspension affecting the initial release of BSA from the microparticles, as discussed below. Protein-loaded PLGA microparticles size can be tuned using homogenizer speed. The homogenizer speed was fixed at 12 000 rpm to obtain microparticles of average size 3 ± 0.85 μm, suitable for injectable protein depots, using smaller diameter needle with better patient comfort.[53] The surface morphology of the protein-loaded microparticles prepared by different methods shows smooth surface without any noticeable pore. Moreover, high protein-loaded (8% BSA) microparticles using our sg−o−w method results in spherical microparticles with smooth surface morphology (data not shown).

We probed the distribution of proteins in the microparticle matrix prepared by different methods. The distribution of protein is important to predict protein-loading capacity, stability, and release profiles. As expected, conventional emulsion methods result in peripheral and occasional clumped distribution of proteins in the microparticle matrix due to possible separation of proteins in the aqueous phase from the hydrophobic polymer.[54] In contrast to that, uniform distribution of the protein in sg−o−w microparticles is mainly due to the protein-in-solid-SGnP (without aqueous phase) and its coating of AOT surfactant on it, which facilitates uniform distribution of protein−SGnP throughout the hydrophobic polymer−solvent matrix (see Figure 2c,d). As expected, distribution of dual proteins (SGnP-mediated loading) in the microparticle matrix (representing double protein-encapsulated system) confirms their uniform, yet distinct, distribution of individual protein-dye (Figure 2e), which is necessarily needed to preserve specific proteins by providing unique microenvironment specific to that protein, and thus their bioactivity during storage and processing. However, it is not possible to load multiple proteins in the microparticle in the conventional w−o−w method, where an individual protein is distributed throughout the polymer matrix distinctly, yet surrounded by protein-specific microenvironment, essential to provide stability to the protein during processing and in vitro and in vivo storage. Note that our sg−o−w method will allow the loading of three or more proteins in a single microparticle

system by just using individual protein−SGnP system, where each protein remains within their unique microenvironment in the microparticle's polymer matrix, which is unique for our SGnP system.

Protein-loaded microparticles prepared by conventional methods (w−o−w, w−o−o) result in low encapsulation efficiency as well as low loading capacity of proteins (Table 1) mainly due to possible separation of the protein and polymer phase (as observed in confocal microscopy images, Figure 2a) and loss of protein during the secondary emulsion process.[55] Conversely, high encapsulation efficiency by SGnP-mediated methods in comparison to encapsulation by conventional methods (protein-in-buffer) can be attributed to SGnP-mediated uniform nanodistribution of protein into the polymer matrix, restricting protein clump formation (due to phase separation) and their loss during secondary emulsion process. It is important to load proteins into the microparticles as high as 3 to 12% (w/w) as reported to make protein depots with extended sustained-release properties.[56] However, ∼16% rhGH loading (target) was reported into PLGA matrix in Nutropin Depot prepared by the conventional w−o−w method. Note that in such conventional method, most of the encapsulated protein fraction (>70%) loses its activity during the encapsulation process as shown in Figure 4. Thus, the amount of effective active protein in such formulations should be around <5% (loading capacity). If there is no significant activity loss during processing/storage, one can expect that low amount of protein loading (<5%) into microparticles (with low loading capacity) should be sufficient for the preparation of long-term delivery protein depot. Thus, we anticipated that using our modified SGnP system (with maximum protein molecules, trehalose/protein ratio 20:1), we can prepare longer release protein depot with target protein loading capacity (<5%). However, in our sg−o−w method, loading of protein more than 5% (w/w) into the polymer microparticles is possible by simply increasing the amount of modified protein−SGnP in the specific amount of polymer. However, one can expect that the increase in the amount of SGnP into the polymer matrix may have detrimental effect on the release profile. This may be due to the possibility of formation of a nanoporous polymer matrix when particles come in contact with an aqueous medium, particularly in the case of a higher amount of SGnP. Our effort to make high BSA-loaded microparticles up to 15% BSA using our modified BSA−SGnP shows relatively higher encapsulation efficiency and loading capacity compared to the conventional w−o−w method (see the Supporting Information Table S7). The sg−o−w particles with theoretical protein loading up to 8% shows moderate release (26%) at 24 h followed by sustained release of protein in contrast to 80% release of BSA at 24 h from w−o−w particles (see the Supporting Information Table S7). However, as expected, 15% theoretical loading particles prepared by our sg−o−w method result in high release of BSA (91%) within 24 h, which is similar to that by w−o−w particles (release profiles from different formulation discussed below).

The sustained release of protein from the microparticle is necessary for any effective protein depot system. Sustained release can be accomplished by modulating the diffusion rate of the encapsulated protein, which depends on the extent of molecular dispersion of protein in the matrix, biodegradability of the polymers, diameters and porosities of the microparticles, and protein−polymer interaction.[57] As expected from the protein distribution pattern in the microparticles (Figure 2)

prepared by the conventional emulsion process, it shows burst release due to instant release of protein segregated at the particle periphery. Many approaches have been considered to control protein release kinetics, including tailoring of protein−polymer chemical interactions,[58] use of additional matrix materials,[59,60] and secondary incorporation of proteins into microspheres.[61] However, the release profile of individual proteins (BSA, FGF-2, and EGF) from the sg−o−w micro-particle shows low initial release characteristics mainly due to the excellent dispersion properties of protein−SGnP in the polymer matrix (Figure 2c,d). Similar very low initial release of both EGF and FGF-2 proteins from dual protein-loaded microparticle is observed as SGnP resulted in uniform distribution of individual proteins (EGF or FGF-2) as distinct nanoentities throughout the microparticle matrix (Figure 2e showing uniform distribution of protein-red−SGnP and protein-green−SGnP). The initial release of BSA from low theoretical protein-loading particles (0.008 to 0.05%, mimick-ing typical loading of GF required for their local delivery for tissue engineering application[62]) (Figure 3a) expectedly shows high initial burst release (55 to 74%) for conventional w−o−w particles. The high burst release is due to the preferential segregation of protein close to the particle periphery leaving less amount of protein inside the polymer matrix. Conversely, very low release of BSA (7%) from similar low theoretical protein-loaded sg−o−w is due to the uniform distribution of BSA−SGnP (∼23 nm size) within the microparticle matrix. The initial release of 7 to 10% of protein from sg−o−w particles could be explained from a simple geometric consideration, as depicted in Figure 3e,f. Given an average microparticle diameter of 3 ± 0.85 μm and a homogeneous distribution of nanoparticles with diameters of 23 ± 0.5 nm, approximately 8 to 10% of the particles will have their centers located within one particle radius from the surface of the microparticles. In other words, these protein−SGnPs will have some direct exposure to the surrounding medium, as they are not being shielded by a significant amount of PLGA. Conversely, relatively higher initial release of 15−21% of BSA from the high protein-loaded (1−5% w/w) sg−o−w microparticles may be explained by the presence of agglomerated bigger BSA−SGnP (Figure S2). As expected, their peripheral distribution results in an initial release (15%) higher than 7−10%, calculated from the above geometric consideration of ∼50 to 100 nm protein−SGnP. Note that to maximize the protein loading (5−15% w/w), we used a lower amount of trehalose for a specific amount of BSA (i.e., BSA/trehalose = 1:20), which resulted in agglomerated protein−SGnP of size 50 to 100 nm (see Figure S2). The sg−o−w (1% theoretical loading) formulation shows higher initial release (21%) than 5% protein-loaded sg−o−w particles. This may be due to loading higher amount (80% w/w) of nanosized SGnP (∼30 nm) into the polymer matrix (see the Supporting Information Table S4). However, for low-protein-loaded microparticles, we have used the protein−SGnP system with a higher amount of trehalose (trehalose/protein; 200:1), resulting in monodispersed protein−SGnP of ∼23 nm in suspension (see Figure S2) and thus, initial release of ∼7−10%. Individual GFs (EGF or FGF-2) release profiles from two type of particles (sg−o−w and w−o−w), as expected, shows results similar to their low protein-loaded BSA particles. Note that NanoOrange was used to quantify the EGF or FGF-2 (active and inactive fraction) in the release medium (Figure 3c). In case of the dual protein-loaded system (Figure 3d), as

expected the release profiles of the active fraction of the individual protein (EGF or FGF-2) from sg−o−w microparticles (measured by ELISA, active fraction of individual EGF or FGF-2) as well as total protein (measured by NanoOrange total EGF + FGF-2 including active + inactive fraction of EGF/FGF-2) follow release characteristic similar to that for low-protein-loaded sg−o−w microparticles, that is, individual protein−SGnP (BSA/EGF/FGF-2)-loaded microparticles (Figure 3a,c). Cumulative initial release of ~6% of two proteins (active + inactive fraction of EGF and FGF-2) should be explained by this geometric consideration of arrangement of 23 nm GF-SGnP close to the periphery of sg−o−w microparticles. Interestingly, release profiles of active fraction of individual GF, EGF, and FGF-2 from the conventional (w−o−w) dual protein microparticles measured by ELISA show low initial burst release (<20%) followed by sustained release, which is contradictory to release profiles of BSA/EGF/FGF-2 from the w−o−w single protein microparticles system. This discrepancy is due to the presence of inactive fraction (denatured/miss-folded) GFs in the release medium (~63%) which cannot be detected by ELISA, leading to misinterpretation/wrong-presentation of release profiles of GF from the polymeric microparticles often reported in the literature,[10] claiming burst-free sustained release. Note that >70% inactive protein fraction is present in w−o−w microparticles. It is further confirmed by the fact that the release profile of total protein (active and inactive fraction of both EGF and FEF-2) from w−o−w particles measured by NanoOrange (Figure 3d) shows similar release profiles of individual protein (BSA/EGF/FGF-2) from conventional w−o−w microparticles, that is, ~50% initial release. Note that the estimation of inactive fraction of individual GF (FGF-2/EGF) in the released medium of dual-GFs-loaded particles is not possible using NanoOrange. However, an estimation has been provided based on the active and inactive fractions of EGF or FGF-2 estimated in the released samples from individual-GF-loaded microparticles in Figure 4b (see the Supporting Information Table S8). Thus, total individual EGF/FGF-2 (active and inactive fraction) release from the dual-GF-loaded particles should be similar to the total GFs release profile in Figure 3d, that is, ~50% initial release of FGF-2/EGF from w−o−w particles. It is to be noted that EGF and FGF-2 show slightly different release profiles from any particles (w−o−w or sg−o−w), where EGF follows slower release than FGF-2. The slight difference in the release pattern between an individual protein, BSA/EGF/FGF-2, from any specific type of particles (w−o−w or sg−o−w) may be attributed to size and structural (specific amino acid sequence, etc.) differences of the individual protein and specific interaction between the protein and polymer matrix (PLGA molecule having carboxyl terminal group) possibly affecting their diffusion rate. It is important to note that SGnP-mediated protein (e.g., GFs)-loaded microparticles, as expected, show very low initial release followed by sustained release of protein for more than 1 month (only 30 to 40% release of BSA) as shown in their release profiles. To account for the residual protein (BSA) in the microparticle after certain day of release, we tried to extract protein from the released (for 15 days) particles. We have estimated the percent (%) of protein recovery after 2 weeks of in vitro release of BSA from the different microparticles (target theoretical loading of 1 and 5% of w−o−w and sg−o−w microparticles) (see the Supporting Information Figure S8). The result indicates 80−

90% recovery of unreleased BSA from all formulations, confirming its possible longer release.

For the development of a protein depot, it is essential to preserve the activity of the encapsulated protein during microparticle preparation for delivery of the proteins in their active form from the protein depot. Stability of proteins in the PLGA microparticles has been considered as the most significant issue impeding the development of the PLGA depot of proteins.[63] We have used three model proteins; namely HRP, FGF-2, and EGF to comparatively study process-related activity loss of protein during preparation of microparticles by SGnP-mediated or conventional emulsion. Enzymatic activity assay was performed to estimate the active HRP in the different microparticles (w−o−w and sg−o−w). Although the ELISA measured the antibody-binding activity of the protein, but the ELISA activity has been reported to correlate with the bioactivity of protein.[64] We also observed similar correlation of FGF-2 activity measured by ELISA and the HGF-proliferation assay[65] (Figure 4c,d). As expected, we observed significant process-related protein activity loss (>70%) when the protein (HRP, FGF-2, and EGF) is encapsulated into microparticles from buffer in the conventional emulsion method due to mechanical and aqueous−organic interfacial stresses (substantial miss-folding and subsequent denature).[38] On the other hand, minimum process-related protein activity loss (<20% protein) observed in the SGnP-incorporated microparticle system, attributes to robust protection of the SGnP system from organic solvent exposure and interfacial stresses.[47] SGnP also provides an environment of sugars that stabilizes the protein against degradation during further processing and storage.[66] One can expect that when a protein undergoes possible miss-folding/denaturation during the microparticle fabrication process, it cannot bind to its native structure's specific antibody in ELISA as well as cell surface receptors. Thus, negligible variation in the remaining active FGF-2 in the microparticle, as measured by ELISA and proliferation of HGF cells, confirms the correlation between the two activity assays. We anticipated the bioactivity of EGF released from different microspheres to be similar to its antibody-binding activity measured by ELISA. There is a uniformly high degree of protection of proteins from process-related stress (mechanical agitation and interfacial stress) by the SGnP system. In this study, we only measured the activity of eluted fractions of GFs up to day 10 of their release, showing presence of >80% active protein when protected within our SGnP matrix. However, the protein may denature/loose activity in the microenvironment of a hydrophobic polymer matrix until the point when the protein is released in vivo (in vivo storage stability).[10,67] This warrants further investigation of in vivo storage stability of protein inside the PLGA microparticles in an in vivo environment. Several approaches have been considered to overcome the deleterious physical−chemical event occurring during in vivo storage such as use of a protein-stabilizing excipient (heparin),[54,68,69] pH-controlling molecules, and so forth.[43] One can expect that these approaches can be easily implemented within our SGnP matrix system to achieve the in vivo storage stability that may be specific for any protein−polymer system.

Protein stability during storage of the protein depot is vital for effectiveness in a long-term release and vital for manufacturing and off-the-shelf use. We studied the storage stability of the encapsulated protein in the microparticles using

HRP as the model protein system. We did not use FGF-2/EGF for this study, as they are expensive. Unprotected (w−o−w and w−o−o microparticles) and SGnP-protected (sg−o−w and sg−o−o) HRP enzymatic activity in microparticles after storage at room temperature (25 °C) decays to its 50% at 5 days and 70 days, respectively (Figure 5). Excellent storage stability of HRP when protected by the SGnP system can be attributed to the stabilization of proteins in the glassy-trehalose matrix, which protects proteins from any conformation change and chemical and physical degradation.[47,70] This protection ability of the SGnP system becomes stronger with lowering the temperature compared to unprotected protein. It is expected that the elevation in ambient temperature, humidity, and change in pH account for storage-related stresses on the encapsulated proteins.[71] Thus, we observed only <2% SGnP-protected HRP activity loss after 100 days of storage at −80 °C compared to >70% protein activity loss in unprotected-HRP system. Note that protein depot loaded with SGnP-protected protein could be stored at room temperature for at least a month and several months at −80 °C with <20% loss of protein activity. However, the storage stability at room temperature (25 °C) as well as 4 °C can be further improved significantly by changing the storage condition such as storage at dry condition (moisture free environment) as the sugar-glassy matrix is susceptible to moisture.[72] It is obvious from the results that even if a large amount of active, unprotected protein is introduced into microparticles by the conventional emulsion method, it would degrade entirely in just a few days, making a protein depot with long term storage and off-the-shelf use impossible.

Ex vivo functional assay was performed to check the potentiality of our SGnP-mediated dual protein-loaded protein depot for "cancer stem cell mammosphere" formation. The conventional mammosphere assay involves incubation of optimum density of cancer cells in a low adherence plate and serum-free culture medium supplemented with growth factors (EGF and FGF-2, 10−30 ng/mL),[73] which require replenishment at defined intervals to maintain constant and active concentration of growth factors. A protein depot such as our SGnP-mediated dual protein-loaded microsphere should be ideal to deliver and maintain active concentration of both proteins in the culture medium for at least 7 days (>10 ng/mL) (see the Supporting Information Figure S9). MCF-7 cells are composed of populations that are characterized by CD44⁻/CD24⁺ and CD44⁺/CD24⁺ phenotypes.[74] Breast cancer cell population of CD44⁺/CD24⁻/low is considered having stem cell-like properties and high tumorigenicity.[75] Hence, we have analyzed the expression of the CD24 marker in the cancer cell line as well as mammospheres in order to check the enrichment of CSCs. Figure 6 represents the mammospheres and their CD24 expression, generated in the presence of free growth factors and growth factor-loaded protein depot, with respect to the MCF-7 cell line. Even though the number of spheres formed in both groups has been found to be similar, the mammospheres generated with the protein depot exhibited an increase in the cell population having decreased expression of CD24 compared to those generated in the presence of free growth factors. It is to be noted that the SGnP-mediated dual growth factors-loaded (FGF-2 and EGF) microparticles were used for stem cell mammospheres formation after 25 days of storage at 4 °C. Meanwhile, as expected, we found negligible amount (<10% of original loading) of residual active protein in the protein depot prepared by conventional methods under

similar conditions (loading and storage) and hence, we did not use those microparticles for the generation of mammospheres. It is expected that the SGnP system protects proteins during processing and storage of microparticles and facilitates high encapsulation and sustained release of protein(s) in their active forms (>10 ng/mL throughout the experiment time) compared to fluctuation of GFs concentration (<10 ng/mL at day 3 or day 7) in the externally added GFs well (see Figure S9). Relatively higher transformation efficiency of cancer stem cells cultured in the presence of the protein depot sample may be due to maintenance of the active growth factor (FGF-2 and EGF) concentration above the effective dose (>10 ng/mL) required for stem cell formation. Cancer stem cell formation by our protein depots confirmed the preservation of the bioactivity of the proteins within the particles and their sustained release in active form over the course of the experiment, which closely mimics the in vivo application of the protein depot.

5. CONCLUSIONS

Microparticle protein depot developed using the conventional emulsion-based method has failed in clinic due to its low loading efficiency, high burst release, and protein denaturation during microsphere preparation. It is crucial for the clinical success of any protein depot to overcome these issues of protein delivery. We have successfully prepared a micro-particle-based protein depot by overcoming the aforementioned challenges of protein delivery. Our previously developed novel nanoencapsulation technique of protein into the sugar-glass matrix (SGnP) (with slight modification) was used for encapsulation of single and multiple proteins in the microparticle, resulting in high encapsulation efficiency, excellent protection from process-related stresses, very good storage stability, and burst-free sustained release. Our modified SGnP system allows to make protein depots with theoretical protein loading up to 8%, which shows low initial release (up to 15%), higher loading capacity (4.5%), sustained release, and excellent storage stability. The prepared PLGA microparticle-based protein depot can deliver proteins (BSA, EGF, and FGF-2) beyond one month. Once the protein is encapsulated in SGnP, the SGnP is robust to protect it from a range of organic solvents (PI < 5). Thus, protein depots with different polymer systems (other than PLGA to avoid possible in vivo toxicity from acidic degradable product) and single/multiple proteins can be prepared. It is important to note that during the past 15 years, many approaches have been developed to ameliorate the above said challenges individually or together. However, these different approaches, which may be specific for particular protein−polymer system, can be easily implemented within our SGnP system for improved result. As an example, heparin has been used to provide stability of proteins (within polymer matrix) until the point of release of proteins in vivo. The SGnP matrix can be modified by the incorporation of heparin, which may provide stability of proteins in vivo. Our current effort is preparation and characterization (physical and biological) of microparticles protein depots of clinically relevant therapeutic protein such as coagulation factor VII, human recombinant growth hormone, and interferon B.

ASSOCIATED CONTENT

ⓢ Supporting Information

The Supporting Information is available free of charge at https://pubs.acs.org/doi/10.1021/acs.molpharmaceut.9b01022.

Standard plot for total and active protein (BSA, HRP, FGF-2, and EGF); protein quantification using micro BCA assay kit, enzymatic activity using OPD substrate, NanoOrange kit and sandwich ELISA; cryo-SEM images of BSA–SGnP with different amount of trehalose: BSA; SEM micrographs of PLGA microparticles prepared by different emulsion techniques (w–o–w, sg–o–w, w–o–o, and sg–o–o) and their corresponding size distribution; FITC–BSA distribution within the particles prepared by w–o–o and sg–o–o emulsion techniques; cumulative release of BSA from PLGA microparticles prepared by the w–o–o method with theoretical target loading of protein at 1% (w/w) and 5% (w/w); FGF-2GF dose-dependent proliferation of HGF cultured for 48 h in the presence of FGF-2; 3 months storage stability of HRP in the different microparticles (w–o–o and sg–o–o) stored at three different temperature (25, 4, and −80 °C); recovery of unreleased BSA from particles prepared by w–o–w and sg–o–w emulsion techniques after 14 days; FGF-2 and EGF concentration in the stem cell culture medium at day 3 and day 7; different ingredients used in the preparation different protein-loaded SGnPs; formulation and constituent details uses for the preparing microparticles by the w–o–w, w–o–o, sg–o–w, and sg–o–o methods; summary of the encapsulation efficiency, loading capacity (target and actual), and burst release of high BSA-loading formulation (1 and 5%) from w–o–o and sg–o–o; summary of the encapsulation efficiency, loading capacity (target and actual), and burst release of high BSA loading formulation (8 and 15%) w–o–w and sg–o–w microparticles; summary of the release profile of FGF-2 and EGF as single and dual protein loading via w–o–w and sg–o–w emulsion; and active fraction of the GF is quantified by respective ELISA and the total protein (active and inactive fractions) is quantified by NanoOrange (PDF)

AUTHOR INFORMATION

Corresponding Author

*E-mail: jgiri@iith.ac.in. Phone: +91-9701277518.

ORCID ⓘ

Arpan Pradhan: 0000-0003-3924-745X

Jyotsnendu Giri: 0000-0002-2313-4912

Notes

The authors declare no competing financial interest.

ACKNOWLEDGMENTS

REFERENCES

(1) Lagassé, H. A. D.; Alexaki, A.; Simhadri, V. L.; Katagiri, N. H.; Jankowski, W.; Sauna, Z. E.; Kimchi-Sarfaty, C. Recent Advances in (Therapeutic Protein) Drug Development. *F1000Research* **2017**, *6*, 113.

(2) Patel, A.; Cholkar, K.; Mitra, A. K. Recent Developments in Protein and Peptide Parenteral Delivery Approaches. *Ther. Delivery* **2014**, *5*, 337−365.

(3) Li, S.-C.; Jin, J.; Sklar, G. E.; Min Sen Oh, V. Factors Affecting Therapeutic Compliance: A Review from the Patient's Perspective. *Ther. Clin. Risk Manage.* **2008**, *4*, 269−286.

(4) Buse, J. B.; Drucker, D. J.; Taylor, K. L.; Kim, T.; Walsh, B.; Hu, H.; Wilhelm, K.; Trautmann, M.; Shen, L. Z.; Porter, L. E.; et al. DURATION-1: Exenatide Once Weekly Produces Sustained Glycemic Control and Weight Loss Over 52 Weeks. *Diabetes Care* **2010**, *33*, 1255−1261.

(5) Kumar, T. S.; Soppimath, K.; Nachaegari, S. K. Novel Delivery Technologies for Protein and Peptide Therapeutics. *Curr. Pharm. Biotechnol.* **2006**, *7*, 261−276.

(6) Bock, N.; Dargaville, T. R.; Woodruff, M. A. Controlling Microencapsulation and Release of Micronized Proteins Using Poly(Ethylene Glycol) and Electrospraying. *Eur. J. Pharm. Biopharm.* **2014**, *87*, 366−377.

(7) Wan, F.; Maltesen, M. J.; Andersen, S. K.; Bjerregaard, S.; Baldursdottir, S. G.; Foged, C.; Rantanen, J.; Yang, M. Modulating Protein Release Profiles by Incorporating Hyaluronic Acid into PLGA Microparticles Via a Spray Dryer Equipped with a 3-Fluid Nozzle. *Pharm. Res.* **2014**, *31*, 2940.

(8) Selcan Gungor-Ozkerim, P.; Balkan, T.; Kose, G. T.; Sezai Sarac, A.; Kok, F. N. Incorporation of Growth Factor Loaded Microspheres into Polymeric Electrospun Nanofibers for Tissue Engineering Applications. *J. Biomed. Mater. Res., Part A* **2014**, *102*, 1897−1908.

(9) Rodness, J.; Mihic, A.; Miyagi, Y.; Wu, J.; Weisel, R. D.; Li, R.-K. VEGF-Loaded Microsphere Patch for Local Protein Delivery to the Ischemic Heart. *Acta Biomater.* **2016**, *45*, 169−181.

(10) Schwendeman, S. P.; Shah, R. B.; Bailey, B. A.; Schwendeman, A. S. Injectable Controlled Release Depots for Large Molecules. *J. Controlled Release* **2014**, *190*, 240−253.

(11) Patel, A.; Patel, M.; Yang, X.; Mitra, A. Recent Advances in Protein and Peptide Drug Delivery: A Special Emphasis on Polymeric Nanoparticles. *Protein Pept. Lett.* **2014**, *21*, 1102−1120.

(12) Ye, M.; Kim, S.; Park, K. Issues in Long-Term Protein Delivery Using Biodegradable Microparticles. *J. Controlled Release* **2010**, *146*, 241−260.

(13) Pagels, R. F.; Prud'homme, R. K. Polymeric Nanoparticles and Microparticles for the Delivery of Peptides, Biologics, and Soluble Therapeutics. *J. Controlled Release* **2015**, *219*, 519−535.

(14) Iqbal, M.; Zafar, N.; Fessi, H.; Elaissari, A. Double Emulsion Solvent Evaporation Techniques Used for Drug Encapsulation. *Int. J. Pharm.* **2015**, *496*, 173−190.

(15) Wei, Y.; Wang, Y.; Kang, A.; Wang, W.; Ho, S. V.; Gao, J.; Ma, G.; Su, Z. A Novel Sustained-Release Formulation of Recombinant Human Growth Hormone and Its Pharmacokinetic, Pharmacodynamic and Safety Profiles. *Mol. Pharm.* **2012**, *9*, 2039−2048.

(16) Govardhan, C.; Khalaf, N.; Jung, C. W.; Simeone, B.; Higbie, A.; Qu, S.; Chemmalil, L.; Pechenov, S.; Basu, S. K.; Margolin, A. L. Novel Long-Acting Crystal Formulation of Human Growth Hormone. *Pharm. Res.* **2005**, *22*, 1461−1470.

(17) Genentech: Press Releases|Tuesday, Jun 1, 2004. https://www.gene.com/media/press-releases/7447/2004-06-01/genentech-and-alkermes-announce-decision (accessed Nov 14, 2019).

(18) Yuan, W.; Cai, Y.; Xu, M.; Yuan, M.; Liu, Z. Developments in Human Growth Hormone Preparations: Sustained-Release, Prolonged Half-Life, Novel Injection Devices, and Alternative Delivery Routes. *Int. J. Nanomed.* **2014**, *9*, 3527.

(19) Park, K.; Skidmore, S.; Hadar, J.; Garner, J.; Park, H.; Otte, A.; Kwan Soh, B.; Yoon, G.; Yu, D.; Yun, Y.; et al. Injectable, Long-Acting PLGA Formulations: Analyzing PLGA and Understanding Microparticle Formation. *J. Control. Release* **2019**, *304*, 125.

(20) Wei, Y.; Wang, Y.; Kang, A.; Wang, W.; Ho, S. V.; Gao, J.; Ma, G.; Su, Z. A Novel Sustained-Release Formulation of Recombinant Human Growth Hormone and Its Pharmacokinetic, Pharmacodynamic and Safety Profiles. *Mol. Pharm.* **2012**, *9*, 2039−2048.

(21) Wu, J.; Williams, G. R.; Branford-White, C.; Li, H.; Li, Y.; Zhu, L.-M. Liraglutide-Loaded Poly(Lactic-Co-Glycolic Acid) Microspheres: Preparation and in Vivo Evaluation. *Eur. J. Pharm. Sci.* **2016**, *92*, 28−38.

(22) Esparza, I.; Kissel, T. Parameters Affecting the Immunogenicity of Microencapsulated Tetanus Toxoid. *Vaccine* **1992**, *10*, 714−720.

(23) Ruiz, J.; Tissier, B.; Benoit, J. Microencapsulation of Peptide: A Study of the Phase Separation of Poly(d,l-Lactic Acid-Co-Glycolic Acid) Copolymers 50/50 by Silicone Oil. *Int. J. Pharm.* **1989**, *49*, 69−77.

(24) Wan, F.; Maltesen, M. J.; Andersen, S. K.; Bjerregaard, S.; Foged, C.; Rantanen, J.; Yang, M. One-Step Production of Protein-Loaded PLGA Microparticles via Spray Drying Using 3-Fluid Nozzle. *Pharm. Res.* **2014**, *31*, 1967−1977.

(25) Carrasquillo, K. G.; Stanley, A. M.; Aponte-Carro, J. C.; De Jésus, P.; Costantino, H. R.; Bosques, C. J.; Griebenow, K. Non-Aqueous Encapsulation of Excipient-Stabilized Spray-Freeze Dried BSA into Poly(Lactide-Co-Glycolide) Microspheres Results in Release of Native Protein. *J. Controlled Release* **2001**, *76*, 199−208.

(26) Anandharamakrishnan, C.; Rielly, C. D.; Stapley, A. G. F. Spray-Freeze-Drying of Whey Proteins at Sub-Atmospheric Pressures Spray-Freeze-Drying of Whey Proteins at Sub-Atmospheric Pressures Article Published by EDP Sciences. *Dairy Sci. Technol.* **2010**, *90*, 321−334.

(27) Kalantarian, P.; Haririan, I.; Najafabadi, A. R.; Shokrgozar, M. A.; Vatanara, A. Entrapment of 5-Fluorouracil into PLGA Matrices Using Supercritical Antisolvent Processes. *J. Pharm. Pharmacol.* **2011**, *63*, 500−506.

(28) Kluge, J.; Fusaro, F.; Casas, N.; Mazzotti, M.; Muhrer, G. Production of PLGA Micro- and Nanocomposites by Supercritical Fluid Extraction of Emulsions: I. Encapsulation of Lysozyme. *J. Supercrit. Fluids* **2009**, *50*, 327−335.

(29) Yang, W.-W.; Pierstorff, E. Reservoir-Based Polymer Drug Delivery Systems. *J. Lab. Autom.* **2012**, *17*, 50−58.

(30) Wang, Y.; Yang, X.; Liu, W.; Zhang, F.; Cai, Q.; Deng, X. Controlled Release Behaviour of Protein-Loaded Microparticles Prepared via Coaxial or Emulsion Electrospray. *J. Microencapsulation* **2013**, *30*, 490−497.

(31) Yuan, W.; Hong, X.; Wei, L.; Ma, L.; Chen, Y.; Liu, Z. Novel Preparation Method for Sustained-Release PLGA Microspheres Using Water-in-Oil-in-Hydrophilic-Oil-in-Water Emulsion. *Int. J. Nanomed.* **2013**, *8*, 2433−2441.

(32) Lin, Q.; Cai, Y.; Yuan, M.; Ma, L.; Qiu, M.; Su, J. Development of a 5-Fluorouracil-Loaded PLGA Microsphere Delivery System by a Solid-in-Oil-in-Hydrophilic Oil (S/O/HO) Novel Method for the Treatment of Tumors. *Oncol. Rep.* **2014**, *32*, 2405−2410.

(33) Suciati, T.; Howard, D.; Barry, J.; Everitt, N. M.; Shakesheff, K. M.; Rose, F. R. Zonal Release of Proteins within Tissue Engineering Scaffolds. *J. Mater. Sci.: Mater. Med.* **2006**, *17*, 1049−1056.

(34) Ma, G. Microencapsulation of Protein Drugs for Drug Delivery: Strategy, Preparation, and Applications. *J. Control. Release* **2014**, *193*, 324−340.

(35) Vysloužil, J.; Doležel, P.; Kejdušová, M.; Mašková, E.; Mašek, J.; Lukáč, R.; Košťál, V.; Vetchý, D.; Dvořáčková, K. Influence of Different Formulations and Process Parameters during the Preparation of Drug-Loaded PLGA Microspheres Evaluated by Multivariate Data Analysis. *Acta Pharm.* **2014**, *64*, 403−417.

(36) Frokjaer, S.; Otzen, D. E. Protein Drug Stability: A Formulation Challenge. *Nat. Rev. Drug Discovery* **2005**, *4*, 298−306.

(37) Tabata, Y. Significance of Release Technology in Tissue Engineering. *Drug Discov. Today* **2005**, *10*, 1639−1646.

(38) van de Weert, M.; Hennink, W. E.; Jiskoot, W. Protein Instability in Poly (Lactic-Co-Glycolic Acid) Microparticles. *Pharm. Res.* **2000**, *17*, 1159−1167.

(39) Kokai, L. E.; Tan, H.; Jhunjhunwala, S.; Little, S. R.; Frank, J. W.; Marra, K. G. Protein Bioactivity and Polymer Orientation Is Affected by Stabilizer Incorporation for Double-Walled Microspheres. *Elsevier* **2010**, *141*, 168−176.

(40) He, J.-T.; Su, H.-B.; Li, G.-P.; Tao, X.-M.; Mo, W.; Song, H.-Y. Stabilization and Encapsulation of a Staphylokinase Variant (K35R) into Poly(Lactic-Co-Glycolic Acid) Microspheres. *Int. J. Pharm.* **2006**, *309*, 101−108.

(41) Giteau, A.; Venierjulienne, M.; Marchal, S.; Courthaudon, J.; Sergent, M.; Monteromenei, C.; Verdier, J.; Benoit, J. Reversible Protein Precipitation to Ensure Stability during Encapsulation within PLGA Microspheres. *Eur. J. Pharm. Biopharm.* **2008**, *70*, 127−136.

(42) Castellanos, I. J.; Flores, G.; Griebenow, K. Effect of the molecular weight of poly(ethylene glycol) used as emulsifier on α-chymotrypsin stability upon encapsulation in PLGA microspheres. *J. Pharm. Pharmacol.* **2005**, *57*, 1261−1269.

(43) Zhu, G.; Mallery, S. R.; Schwendeman, S. P. Stabilization of Proteins Encapsulated in Injectable Poly (Lactide- Co-Glycolide). *Nat. Biotechnol.* **2000**, *18*, 52−57.

(44) Fonte, P.; Araújo, F.; Seabra, V.; Reis, S.; van de Weert, M.; Sarmento, B. Co-Encapsulation of Lyoprotectants Improves the Stability of Protein-Loaded PLGA Nanoparticles upon Lyophilization. *Int. J. Pharm.* **2015**, *496*, 850−862.

(45) Wang, J.; Wang, B. M.; Schwendeman, S. P. Characterization of the Initial Burst Release of a Model Peptide from Poly(D,L-Lactide-Co-Glycolide) Microspheres. *J. Controlled Release* **2002**, *82*, 289−307.

(46) Reinhold, S. E.; Desai, K.-G. H.; Zhang, L.; Olsen, K. F.; Schwendeman, S. P. Self-Healing Microencapsulation of Biomacromolecules without Organic Solvents. *Angew. Chem. Int. Ed.* **2012**, *51*, 10800−10803.

(47) Giri, J.; Li, W.-J.; Tuan, R. S.; Cicerone, M. T. Stabilization of Proteins by Nanoencapsulation in Sugar-Glass for Tissue Engineering and Drug Delivery Applications. *Adv. Mater.* **2011**, *23*, 4861−4867.

(48) Gao, Y.; Xu, Y.; Land, A.; Harris, J.; Policastro, G. M.; Childers, E. P.; Ritzman, T.; Bundy, J.; Becker, M. L. Sustained Release of Recombinant Human Growth Hormone from Bioresorbable Poly-(Ester Urea) Nanofibers. *ACS Macro Lett.* **2017**, *6*, 875−880.

(49) Issman, L.; Talmon, Y. Cryo-SEM Specimen Preparation under Controlled Temperature and Concentration Conditions. *J. Microsc.* **2012**, *246*, 60−69.

(50) Determan, A. S.; Trewyn, B. G.; Lin, V. S.-Y.; Nilsen-Hamilton, M.; Narasimhan, B. Encapsulation, Stabilization, and Release of BSA-FITC from Polyanhydride Microspheres. *J. Controlled Release* **2004**, *100*, 97−109.

(51) Gustafsson, H.; Küchler, A.; Holmberg, K.; Walde, P. Co-Immobilization of Enzymes with the Help of a Dendronized Polymer and Mesoporous Silica Nanoparticles. *J. Mater. Chem. B* **2015**, *3*, 6174−6184.

(52) Jonchhe, S.; Pandey, S.; Emura, T.; Hidaka, K.; Hossain, M. A.; Shrestha, P.; Sugiyama, H.; Endo, M.; Mao, H. Decreased Water Activity in Nanoconfinement Contributes to the Folding of G-Quadruplex and i-Motif Structures. *Proc. Natl. Acad. Sci. U.S.A.* **2018**, *115*, 9539−9544.

(53) Zhang, S.; Uludağ, H. Nanoparticulate Systems for Growth Factor Delivery. *Pharm. Res.* **2009**, *26*, 1561−1580.

(54) Giteau, A.; Venier-Julienne, M. C.; Aubert-Pouëssel, A.; Benoit, J. P. How to Achieve Sustained and Complete Protein Release from PLGA-Based Microparticles? *Int. J. Pharm.* **2008**, *350*, 14−26.

(55) de Roos, A.; Walstra, P. Loss of Enzyme Activity Due to Adsorption onto Emulsion Droplets. *Colloids Surf., B* **1996**, *6*, 201.

(56) Vaishya, R.; Khurana, V.; Patel, S.; Mitra, A. K. Long-Term Delivery of Protein Therapeutics. *Expert Opin. Drug Deliv.* **2015**, *12*, 415−440.

(57) Fu, Y.; Fu, W. J. Drug Release Kinetics and Transport Mechanisms of Non- Degradable and Degradable Polymeric Delivery Systems. *Expert Opin. Drug Deliv.* **2010**, *7*, 429−444.

(58) Fang, F.; Szleifer, I. Controlled Release of Proteins from Polymer-Modified Surfaces. *Proc. Natl. Acad. Sci. U.S.A.* **2006**, *103*, 5769−5774.

(59) Yuan, W.; Liu, Z. Controlled-Release and Preserved Bioactivity of Proteins from (Self-Assembled) Core-Shell Double-Walled Microspheres. *Int. J. Nanomed.* **2012**, *7*, 257−270.

(60) Feng, F.; Neoh, K. Y.; Davoodi, P.; Wang, C.-H. Fabrication of Double-Wall Microparticles with Protein Loaded in the Hydrophilic Gel Core Using Coaxial Electrohydrodynamic Atomization. *42nd Annual Meeting & Exposition of the Controlled Release Society, At Scotland*, 2015.

(61) Lee, Y.-S.; Johnson, P. J.; Robbins, P. T.; Bridson, R. H. Production of Nanoparticles-in-Microparticles by a Double Emulsion Method: A Comprehensive Study. *Eur. J. Pharm. Biopharm.* **2013**, *83*, 168−173.

(62) Lee, K.; Silva, E. A.; Mooney, D. J. Growth Factor Delivery-Based Tissue Engineering: General Approaches and a Review of Recent Developments. *J. R. Soc. Interface* **2011**, *8*, 153−170.

(63) Fu, K.; Klibanov, A. M.; Langer, R. Protein Stability in Controlled-Release Systems. *Nat. Biotechnol.* **2000**, *18*, 24−25.

(64) Chua, H. Y.; Lui, Y. S.; Bhuthalingam, R.; Agrawal, R.; Wong, T.; Preiser, P. R.; Venkatraman, S. One-Step Solid-Oil-Water Emulsion for Sustained Bioactive Ranibizumab Release. *Expert Opin. Drug Deliv.* **2018**, *15*, 1143−1156.

(65) Takayama, S.-i.; Yoshida, J.; Hirano, H.; Okada, H.; Murakami, S. Effects of Basic Fibroblast Growth Factor on Human Gingival Epithelial Cells. *J. Periodontol.* **2002**, *73*, 1467−1473.

(66) Wang, B.; Tchessalov, S.; Warne, N. W.; Pikal, M. J. Impact of sucrose level on storage stability of proteins in freeze-dried solids: I. correlation of protein-sugar interaction with native structure preservation. *J. Pharm. Sci.* **2009**, *98*, 3131−3144.

(67) Cohen, S.; Bernstein, H. *Microparticulate Systems for the Delivery of Proteins and Vaccines*; Marcel Dekker: New York, 1996.

(68) Lee, J. S.; Go, D. H.; Bae, J. W.; Lee, S. J.; Park, K. D. Heparin Conjugated Polymeric Micelle for Long-Term Delivery of Basic Fibroblast Growth Factor. *J. Controlled Release* **2007**, *117*, 204−209.

(69) Kreitz, M. R.; Domm, J. A.; Mathiowitz, E. Controlled delivery of therapeutics from microporous membranes. II. In vitro degradation and release of heparin-loaded poly(d,l-lactide-co-glycolide). *Biomaterials* **1997**, *18*, 1645−1651.

(70) Olsson, C.; Jansson, H.; Swenson, J. The Role of Trehalose for the Stabilization of Proteins. *J. Phys. Chem. B* **2016**, *120*, 4723−4731.

(71) Zamani, M.; Prabhakaran, M. P.; Thian, E. S.; Ramakrishna, S. Controlled delivery of stromal derived factor-1α from poly lactic-co-glycolic acid core-shell particles to recruit mesenchymal stem cells for cardiac regeneration. *J. Colloid Interface Sci.* **2015**, *451*, 144−152.

(72) Weng, L.; Ziaei, S.; Elliott, G. D. Effects of Water on Structure and Dynamics of Trehalose Glasses at Low Water Contents and Its Relationship to Preservation Outcomes. *Sci. Rep.* **2016**, *6*, 28795.

(73) Iglesias, J. M.; Beloqui, I.; Garcia-Garcia, F.; Leis, O.; Vazquez-Martin, A.; Eguiara, A.; Cufi, S.; Pavon, A.; Menendez, J. A.; Dopazo, J.; et al. Mammosphere Formation in Breast Carcinoma Cell Lines Depends upon Expression of E-Cadherin. *PLoS One* **2013**, *8*, No. e77281.

(74) Sun, H.; Jia, J.; Wang, X.; Ma, B.; Di, L.; Song, G.; Ren, J. CD44+/CD24− breast cancer cells isolated from MCF-7 cultures exhibit enhanced angiogenic properties. *Clin. Transl. Oncol.* **2013**, *15*, 46−54.

(75) Li, W.; Ma, H.; Zhang, J.; Zhu, L.; Wang, C.; Yang, Y. Unraveling the Roles of CD44/CD24 and ALDH1 as Cancer Stem Cell Markers in Tumorigenesis and Metastasis. *Sci. Rep.* **2017**, *7*, 13856.